University of Birmingham

Department of Metallurgy and Materials

Development and characterisation of calcium phosphate glasses and glass-ceramics containing fluorine and titanium

A research project report submitted by

Sukaina Ibrahim

As part of the requirement for the
degree of MRes in Biomaterials

Under the supervision of: Dr Artemis Stamboulis

June 2010

Acknowledgements

I am grateful to my academic supervisor, Artemis Stamboulis, for her presence, support, encouragement and guidance throughout the year. The University of Birmingham for providing me with a tuition scholarship.

Abstract

There is ongoing research into calcium phosphate glasses as possible candidates for use in dental restoration and in the field of bone implants. This is due to the fact that calcium phosphate glasses have many useful properties such as bioactivity, biocompatibility, bioresorbability and non toxicity. However, on the other hand they are also known to fail catastrophically and therefore cannot be used in load bearing applications and are limited as coatings to metallic substrates. Calcium phosphate glasses with different types of oxides such as magnesium, [27-28, 30-34] sodium, [14, 36-40] fluorine [41-42] in the presence of titania have been used in research to investigate whether addition of these oxides can help improve the properties of the glasses. It has been shown that calcium phosphate glasses containing fluorine have shown to produce fluoroapatite which is beneficial as it is known to be one of the ways in order to improve chemical durability of calcium phosphate glass-ceramics. [41-42]

In the present study, type A glass and glass-ceramics demonstrated the effect of TiO_2 addition with reduction of calcium to phosphorus ratio and type B glass and glass-ceramics demonstrated the effect of TiO_2 addition with constant calcium to phosphorus ratio on the structure of fluorine containing calcium phosphate glasses and glass-ceramics. The TiO_2 addition in type A took place in 5 %, 15 % and 20 % molar content of TiO_2 and in type B, TiO_2 was added to glasses in 4.76 %, 11.11 %, 16.66 % and 20 % molar content of TiO_2. FTIR, DSC, XRD, ESEM and TGA (performed only on amorphous glasses) were used to characterise the glasses and glass-ceramics produced.

DSC and density measurements showed that when 15 mol % TiO_2 was added in type A; it caused disruption in the glass network which was confirmed by a reduction in

the Tg. When TiO_2 was added into the glass in type B, there was a general increase in Tg observed which confirmed that TiO_2 might strengthen the glass network.

XRD results showed that in both type A and type B glass-ceramics, crystal phases corresponding to calcium metaphosphate, calcium pyrophosphate and titanium pyrophosphate were present. No phase however corresponding to fluorine was found.

FTIR results of type A and type B glasses showed peaks corresponding to metaphosphate, pyrophosphate and orthophosphate groups. In the FTIR spectra of both the glass-ceramics however, peaks corresponding to the metaphosphate and pyrophosphate groups were decomposed into several narrow peaks.

ESEM images demonstrated the presence of different crystal phases in the glass-ceramics. Titanium pyrophosphate was seen mainly at the surface of the glass-ceramics but in the bulk of the glass-ceramics, crystals corresponding to metaphosphate and pyrophosphate were observed.

TGA and EDX analysis confirmed that unfortunately only some fluorine was retained in the amorphous glass and there was no crystalline phase that contained fluorine.

Table of Contents

CHAPTER 1

1. Introduction

Glass-ceramics are used as biomaterials in two different fields, as durable materials in restorative dentistry and as bioactive materials for the replacement of hard tissue for The crystallisation process must be controlled in order to develop glass-ceramics which possess desirable properties so that they can be utilised in these two different fields. [12] Glass-ceramics which are used as dental restorative materials must possess useful properties such as good aesthetics, high strength and high wear resistance which are crucial in the success of dental restorative materials. Although glass-ceramics exhibit the desired properties for dental restoration, they are known to fail due to them being brittle. Therefore there has been a need, from the very beginning to produce glass-ceramics which have excellent strength and durability in order to prevent failure. Glass-ceramics can also be used as bioactive material to replace hard tissue as bone is susceptible to fracture. Calcium phosphate glasses have attracted a lot of interest as desirable material to replace hard tissue due to the fact that the mineral phase of bone consists of a calcium phosphate phase.

Calcium phosphate glasses have shown to have advantageous properties such as bioactivity, biocompatibility, bioresorbability, biodegradability, osteoconductivity and non toxicity. However calcium phosphate glasses fail due to them being brittle and difficulty to machine and hence are not used in load bearing applications and therefore are used as coatings on metallic substrates. Research into calcium phosphate glasses which contain magnesium, sodium, titania and fluorine have been used to see if the properties of the glass-ceramics can be improved. Recent research has shown that calcium phosphate glasses which contain titania and fluorine have shown to have excellent chemical durability and can have an application as dental filler. [41-42]

1.1 Glass-Ceramics

Glass-ceramics are fine-grained polycrystalline materials produced when glasses of appropriate compositions are heat treated and thus undergo controlled crystallisation to a lower energy crystalline state. [1] As some glasses are very stable and difficult to crystallise whilst others crystallise quickly in a disorderly manner resulting in unwanted microstructures, there are only specific glass compositions which are suitable precursors for glass-ceramics. [2-4]

A glass-ceramic is formed by the heat treatment of glass which results in crystallisation. Crystallisation of glasses is due to the thermodynamic drives for reducing the Gibbs' free energy and the Amorphous Phase Separation (APS) which assists the crystallisation process by easily producing a nucleated phase than it would in the original glass. When a glass is melted, the liquid formed from the melting may suddenly split into two extremely viscous liquids or phases. By cooling the melt to a temperature below the glass transformation region, the result is that the glass is phase separated and this is called liquid-liquid immiscibility and this happens when both the phases are liquid. Therefore, a glass can be considered as a liquid which undergoes a demixing process when it cools. The immiscibility is either stable or metastable depending on whether the phase separation occurs above or below the liquidus temperature respectively. The metastable immiscibility is much more important and has two processes which then cause phase separation and hence crystallisation; nucleation and crystal growth [5-6] and spinodal decomposition. [7]

The first Amorphous Phase Separation process has two distinct stages; Nucleation (when the crystals grow to a visible size on the nucleus) and Crystal growth. Nucleation can either be homogeneous; whereby the crystals form spontaneously within the melt or heterogeneous; whereby crystals form at a pre-existing surface such

as that due to an impurity, crucible wall etc. Frequently, the parent glass composition is purposely chosen to include species which enhance internal nucleation which in many of the cases is required. These species, also called nucleating agents can include metallic agents such as Ag, Pt and Pd or non-metallic agents such as TiO_2, P_2O_5 and fluorides. The second process is spinodal decomposition which involves a gradual change in composition of the two phases until they reach the immiscibility boundary. Both of these processes cause phase separation and therefore lead to crystallisation. As both the processes for Amorphous Phase Separation are different, the glass formed clearly results in having different morphology to each other. [6, 8]

A glass-ceramic is generally not fully crystalline; with the microstructure being 50–95 volume % crystalline with the rest being residual glass. When the glass undergoes heat treatment, one or more crystalline phases may form. Both the compositions of the crystalline and residual glass are different to the parent glass. [8]

In order to develop glass-ceramics that have desirable properties, it is vital to control the crystallisation process so that an even distribution of crystals can be formed. This is done by controlling the nucleation and crystal growth rate. The nucleation rate and crystal growth rate has been shown to be a function of temperature and have been accurately measured experimentally. (Stookey 1959; McMillan 1979, Holand & Beall 2002) [2-4, 9-10]

The aim of the crystallisation process is so that the glass-ceramics has better properties than the parent glass. The glass-ceramic formed depends on efficient internal nucleation from controlled crystallisation which allows the development of fine, randomly oriented grains without voids, microcracks, or other porosity. This

results in the glass-ceramic being much stronger, harder and more chemically stable than the parent glass. [4, 8]

Glass-ceramics are characterised in terms of composition and microstructure because their properties are dependant on these. The ability of a glass-ceramic to be formed as well as its degree of workability depends on the bulk composition which also determines the grouping of crystalline phases which successively govern the general physical and chemical characteristics, e.g. hardness, density, acid resistance, etc. As aforementioned, nucleating agents are used in order for internal nucleation to occur so that the glass-ceramic produced have desirable properties. Microstructure is the key to most mechanical and optical properties; it can promote or diminish the role of the key crystals in the glass-ceramic. [11] The desirable properties obtained from glass-ceramics are crucial in order for them to have applications in the field of biomaterials.

Glass-ceramics are used as biomaterials in two different areas: First, they are used as exceptionally durable materials in restorative dentistry and second, they are applied as bioactive materials for the replacement of hard tissue. Dental restorative materials are materials which restore the natural tooth structure (both in shape and function), exhibit durability in the oral environment, exhibit high strength and are wear resistance. [12]

In order for glass-ceramics to be used for dental applications and be successful as an aesthetic, they must possess high chemical durability, mechanical strength and toughness and should exhibit properties which mimic the natural tooth microstructure. [13] Glass-ceramics allow all these properties to be combined within one material. The glass is converted into a glass-ceramic via controlled crystallisation to achieve the crystal phase wanted and hence the desired properties it could possibly have. Hence,

the glass-ceramic developed allows it to have properties such as low porosity, increased strength, durability, toughness which are all crucial in the field of dental restorations as it prevents restorative failures which are mainly due to stress and porosity which consequently can cause cracks and hence failures. [13]

It took many years of research in order to get a glass-ceramic strong enough to be initially used as a dental reconstructive material. However, over the past few years' research has progressed vastly and now glass-ceramics display good strength, high durability and good aesthetics. The development and processing of glass-ceramics has been focused on particular clinical applications, such as dental inlays, crowns, veneers, bridges and dental posts with abutments. Dental restorative materials must have good marginal fit with the tooth; have biocompatibility, good mechanical properties and low porosity for clinical success. Recent requirement for dental restorative materials is for its appearance to be similar to that of a natural tooth, in terms of translucency and colour. [9]

Although glass-ceramics exhibit the desired properties for dental restoration, their main drawback is that they are brittle which is due to either fabrication defects, which are created during production of the glass-ceramic or surface cracks, which are due to machining or grinding. Therefore, when processing the glass-ceramic, care needs to be taken in choosing the suitable method for production for specific compositions of the glass-ceramic in order to improve their mechanical properties. [14]

Apart from the use of glass-ceramics for dental restorations, they can also be applied as bioactive materials for the replacement of hard tissue. Bone is a complex living tissue which has an elegant structure at a range of different hierarchical scales. It is a composite consisting of collagen, calcium phosphate (in the form of crystallised

hydroxyapatite, HA or amorphous calcium phosphate, ACP) and water. Moreover, proteins, polysaccharides, and lipids are also present in small quantities. Because bone is susceptible to fracture; there has always been a need, since the beginning, for the repair of damaged hard tissue. [15]

There has been a lot of research in the use of biomaterials to replace hard tissue, ranging from using bioinert materials, to bioactive materials such as 'Bioglass' (Hench et al) [16] to 'Apatite-wollastonite (A-W) glass-ceramics (Kokubo et al) [17] and to calcium phosphate materials. Calcium phosphate based materials have received a great deal of attention in this field due to their similarity with the mineral phase of bone. [15]

1.2 Calcium Phosphate Based Materials

The application of calcium phosphates as bone substitute began by Albee (1920), [18] who reported the use of a tricalcium phosphate compound in a bony defect promoted osteogenesis. Many years later, Levitt et al (1969) [19] and Monroe et al (1971) [20] were the first to propose the use of calcium phosphate ceramics for dental and medical implant materials. Subsequently, Hench et al (1971) developed Bioglass® which was a glass-ceramic containing calcium phosphate and demonstrated that it chemically bonded with the host bone through a calcium phosphate rich layer. [16] Furthermore the advantageous properties of calcium phosphate ceramics arose when Nery et al [21] used a calcium phosphate ceramic for implants in surgically produced infrabony defects in dogs. This demonstrated that the calcium phosphate ceramic was nontoxic, biocompatible, and caused no significant haematological changes in the calcium and phosphorus levels. [21] Since then, a great deal of research into calcium phosphate glass-ceramics has been conducted as potentially bone substitutes in dentistry. [22]

.

Materials which are bioactive i.e. the ability to bond to living tissue and enhance bone formation, have the following usual compositional features: (i) SiO_2 contents smaller than 60 mol %, (ii) high Na_2O and CaO content, and (iii) high CaO/P_2O_5 ratio [23]. Although silica based bioactive materials have shown great clinical success in many dental and orthopaedic applications, its insoluble properties have resulted in it as a potential for a long term device and the long term reaction to silica, both locally and systematically has still been unknown. [24] Therefore calcium phosphate glasses without silica have attracted much interest due to their chemical and physical properties. Materials such as Hydroxyapatite, β-tricalcium phosphate, β-calcium pyrophosphate and fluoroapatite are amongst the few that have attracted a lot of interest. They provide a more controlled rate of dissolution compared to silica containing glasses, they are simple, easy to produce, biodegradable, biocompatible, bioresorbable due to their ability to completely dissolve in an aqueous environment and have excellent bioactivity, osteoconductivity as well as not causing an inflammatory response. Due to their properties, especially due to it being bioresorbable, calcium phosphate glasses have been under investigation for several applications in the dental field, particularly as implants. However, only certain calcium phosphate compounds are suitable for implantation, compounds with a Ca/P ratio less than 1 are not suitable for biological implantation due to their high solubility. [15, 24-25]

The structural unit of phosphate glasses is a PO_4 tetrahedron. The basic phosphate tetrahedra form long chains and rings that create the three-dimensional vitreous network. All oxygens in the glass structure are bridging oxygens (BO), and the non-bridging oxygens (NBO) can be formed by including other species such as CaO and Na_2O or MgO. Do to the effects of Ca^{2+}, Na^{2+} and Mg^{2+} in the glass structure; they are defined as glass network modifiers, which form the glassy state and are called ‘invert

glasses.' Hence the structure of phosphate glasses can be described using the Q^n terminology, where n represents the number of bridging oxygen's that a PO_4 tetrahedron has in a P_2O_5 glass, every tetrahedron can bond at three corners producing layers of oxygen polyhedra which are connected together with Van der Waals bonds. When the PO_4 tetrahedron bonds with three bridging oxygens, giving the Q^3 species, it is referred to as an ultraphosphate glass, which usually consists of a 2D network. When it bonds to two bridging oxygen's, usually in a 3D-network it gives the Q^2 species, it is referred to as metaphosphate glass. Further addition gives Q^1 species, also called pyrophosphate glass, which bonds only to one bridging oxygen. Finally, the Q^0 species do not bond to any bridging oxygen and hence is known as an orthophosphate glass. [26]

The main disadvantages of calcium phosphates is their brittleness, difficulty to machine and their potential to fail catastrophically, so they cannot be used in load bearing applications. As a result they are mostly used as coatings on metallic substrates, but calcium phosphate implants also have applications as fillers in polymer matrices, as self setting bone cements and as granules. [15] A great deal of research has been carried out on calcium phosphate glasses and glass-ceramics with addition of certain oxides in order to attempt to improve its properties. They can be categorised into three groups:

1) Calcium phosphates containing Magnesium and Titania
2) Calcium phosphates containing Sodium and Titania
3) Calcium phosphates containing Fluorine and Titania

1) Calcium phosphates containing Magnesium:

A study by Dias et al (2005) [27] studied the crystallisation of the glass-system: $37P_2O_5$–45CaO–5MgO–$13TiO_2$ (Ca/P =0.6) in the pyrophosphate and orthophosphate region, by using TiO_2 as a nucleating agent and MgO as a network modifier. Results showed that they contained four different crystalline phases; two of them, β-CPP and CTP are reported to be biocompatible and bioactive, respectively [28-30]. The biocompatibility of the other two phases, titanium pyrophosphate (TiP_2O_7) and α-CPP have not been clearly reported so far in the literature. It appeared from XRD studies that the formation of α and β-CPP was a simultaneous process by α-CPP crystallising at the same time as β-CPP. [27] A further study by Dias et al (2007) [31] based on the same general composition confirmed these four crystalline phases by XRD patterns. They also reported the chemical degradation of these glass-ceramics to be in between that reported in literature for bioactive ceramics that are clinically used such as HA and TCP. [32] Therefore, these glass-ceramics can be used as bone-graft in certain clinical applications; i.e. cranioplasty, whereby fairly slow resorption of the implant and replacement by bone is necessary. [31]

The addition of magnesium and titanium to calcium phosphate invert glasses was compared by Kasuga et al (1999) [33] using the compositions; 60CaO-$30P_2O_5$-$7Na_2O$-$3TiO_2$ and 60CaO-$30P_2O_5$-$7Na_2O$-3MgO in mol %. (Ca/P = 1). Results had shown that when both compositions were immersed in Simulated Body Fluid (SBF), only the composition containing titania produced a calcium phosphate phase on the surface of the glass-ceramic whereas the magnesium composition did not. [33] This was further confirmed in a later study by Zhang et al who also used TiO_2 as well as Na_2O and MgO in the composition. [34]

Calcium phosphate glasses containing magnesium have the advantage of control over its solubility, as well having good chemical degradation which is reported to be in

between those of bioactive ceramics clinically used, such as TCP and HA.[32] Furthermore they have shown to produce bioactive and biocompatible phases, [27,31, 33-34] However, there has been only little research in addition of magnesium to calcium phosphate glasses when compared with the addition of titania, due to the fact that magnesium containing calcium phosphate glasses do not produce a calcium phosphate phase when immersed in SBF and hence are not useful as bioactive materials for bone implants. Furthermore, titania has been shown to enhance mechanical properties of calcium phosphate glasses as well as improving it's chemical durability and shows other useful properties which will be discussed later on.

2) Calcium phosphates containing Sodium (Na_2O) and Titania (TiO_2):

Kasuga et al, has extensively researched into calcium phosphate glasses in the pyrophosphate region. Kasuga, prepared new types of invert phosphate glasses with compositions of high CaO and low P_2O_5 contents to attain bioactive materials; the glasses consist of PO_4^{3-} (orthophosphate) and/or $P_2O_7^{4-}$ (pyrophosphate) ions without PO_3^{2-} (metaphosphate) ion and the phosphate groups were connected through Ca^{2+} ions, which acted as a network modifier.

Kasuga (1998) for the first time, obtained SiO_2-free calcium phosphate glasses in the pyrophosphate region by introducing small amounts of Na_2O and TiO_2 (totalling 10 mol %.) The majority of his research on calcium phosphate glasses has been based on the composition: $60CaO\text{-}30P_2O_5\text{-}7Na_2O\text{-}3TiO_2$ (Ca/P = 1). [35]

Kasuga's XRD analysis has shown that calcium phosphate glasses containing sodium without titania based on the composition: $60CaO\text{-}30P_2O_5\text{-}10Na_2O$ does not produce a β-TCP phase and only forms β-CPP, β-$NaCaPO_4$ and $4CaO\text{-}3P_2O_5$ (tromelite) phases. [35-36] It has been shown that the addition of titania to the glass $60CaO\text{-}30P_2O_5\text{-}7Na_2O\text{-}$

$3TiO_2$ (Ca/P = 1) resulted in the formation of large crystals of both β-CPP and β-TCP. [35] It was shown that calcium phosphate glasses which have sodium and titania must have a high CaO content (60 mol % or more) in order to contain orthophosphate and pyrophosphate groups (β-TCP and β-CPP) without metaphosphate groups. [36]

Kasuga's (2001) XRD study on machinable calcium pyrophosphate glass-ceramics, had shown that when glass powder compacts of $60CaO\text{-}30P_2O_5\text{-}5TiO_2\text{-}5Na_2O$ (Ca/P = 1) were heated, both β-CPP and β-TCP were observed and with increasing temperature, the peak intensities of β-CPP decreased slightly, although β-CPP crystal could not be melted below ≈1350°C. [37] Kasuga et al's study on calcium phosphate glass-ceramics for bioactive coating on a titanium alloy revealed that the surface of the coating of a titanium alloy was made up of mainly β-TCP and β-CPP crystalline phases. It also showed that $60CaO\text{-}30P_2O_5\text{-}7Na_2O\text{-}3TiO_2$ glass-ceramic layer has a greater amount of β-TCP compared with $50CaO\text{-}40P_2O_5\text{-}7Na_2O\text{-}3TiO_2$ glass-ceramic and that $(Ca_{0.5},Na)Ti_2(PO_4)_3$ crystals also precipitated possibly due to the higher Ca/P. [38]

Differential thermal analysis (DTA) from Kasuga's studies (1998, 1999) based on the composition $60CaO\text{-}30P_2O_5\text{-}7Na_2O\text{-}3TiO_2$ (Ca/P = 1) observed a small shrinkage of the glass powder compacts at 600-800°C which was believed to be due to the viscous flow of the glass powders. Two crystallisation peaks, Tp's were observed between 630-750°C and a melting temperature, Tm at ≈ 800°C which was thought to be due to the partial melting of the crystalline phase. [33, 35] Kasuga's further studies (2002, 2003) [38-39] on calcium phosphate glasses and their coating on titanium alloys based on the same composition and another, $50CaO\text{-}40P_2O_5\text{-}7Na_2O\text{-}3TiO_2$ revealed very similar DTA results in both exothermic and endothermic peaks and also had shown that both powder compacts sinter at 800°C. [38-39] A study on machinable calcium

pyrophosphate glass-ceramics, (2001) [37] based on the composition: 60CaO-30P_2O_5-5TiO_2-5Na_2O (Ca/P = 1) suggested that crystallisation of the glasses occur at 640-730°C resulting in the formation of β-CPP and β-TCP crystalline phases with a residual phosphate glassy phase containing TiO_2. [35] The partial melting of the precipitated CPP phase in the crystallised product occurred by a reaction with the glassy phase, when the temperature was increased over 780°C. The viscous flow of the formed melt around 800°C, resulted in the sintering of the powders. Although the densification was almost completed at 850-870°C, the partial melting of the CPP phase continues gradually. At temperatures above 900°C, there was no crystallisation of new phases and no phase transformation of the precipitated crystals was observed. It was thought that the gases involved in the melt may have been emitted to form pores. Therefore, the optimum heating temperature for the glass was determined to be 850°C. [37]

Results from Kasuga's FTIR study showed peaks at 960-1060cm^{-1} which correspond to PO_4^{3-} group of calcium orthophosphates such as HA and a peak at ≈3500cm^{-1} corresponding to the OH group; both peaks were increased after soaking in SBF. [33, 35]

Based on another study [36] on the composition, xCaO-(90-x)P_2O_5-3TiO_2-7Na_2O, when x = 45 (Ca/P = 0.5), Raman spectra showed strong peaks at ≈700cm^{-1} and ≈1170cm^{-1}, which were due to the PO_3 group. [40] In the glass x =55, peaks corresponding to the pyrophosphate group were observed. When the CaO content in the glass increased above 58 mol %, it was confirmed that small amounts of Na_2O and TiO_2 had no long chain phosphate structure and were invert glasses with orthophosphate and pyrophosphate groups. [36] Furthermore the Raman spectra showed that increasing the amount of TiO_2 with decreasing Na_2O in the composition: 60CaO-30P_2O_5-yTiO_2-(10-y)Na_2O caused an increase in the intensity of peaks

corresponding to TiO_4 and to TiO_6. [36] Furthermore, Raman spectra have shown that in the composition, $60CaO\text{-}30P_2O_5\text{-}7Na_2O\text{-}3TiO_2$ a peak corresponding to PO_4: (orthophosphate group) as well as P_2O_7 (pyrophosphate group) were observed and that no metaphosphate group was detected. [38]

In another study by Navarro et al (2003), [14] on the glass-system, P_2O_5–CaO–Na_2O (Ca/P = 0.5), with titania addition Raman spectra showed that TiO_2 free glasses displayed the characteristic shifts of metaphosphate glasses: the PO_2 asymmetric stretch at $\approx 1260cm^{-1}$, the PO_2 symmetric stretch at $\approx 1170cm^{-1}$ and the P-O-P symmetric stretch near $690cm^{-1}$ both of which corresponded to metaphosphate groups, and the PO_3 symmetric stretch at $1040cm^{-1}$ corresponding to pyrophosphate groups. The rest of the glasses which had TiO_2, contained the peaks aforementioned as well as new bands; TiO_5 stretch at $900cm^{-1}$ and the TiO_6 units stretch at $630cm^{-1}$. It was also observed that these new bands increased in intensity as the amount of TiO_2 added to the glasses increased. [14]

Kasuga's SEM observations based on the composition: $60CaO\text{-}30P_2O_5\text{-}7Na_2O\text{-}3TiO_2$ showed that due to the different atomic number contrast of phases precipitated, there were bright and dark portions in the images of the glass-ceramic. Phases A and B were bright portions whereas C was the dark portion. A and B phases consisted of calcium phosphates with small amounts of Na. Phase A was larger in Ca content than phase B and hence, phase A corresponded to β-TCP and phase B to β-CPP. Phase C, the dark portion contained larger amounts of Ti with Na with lower Ca content than phases A and B. Phase C is believed to be caused by the partial melting due to the densification of the glass powders. Therefore the bright portions observed were the calcium phosphate crystalline phases and the dark portions were the glassy phases containing TiO_2 and Na_2O. [33, 35]

Kasuga's study (2001) [37] whereby he first reported machinable silica free glass-ceramics showed that based on the composition: $60CaO\text{-}30P_2O_5\text{-}5TiO_2\text{-}5Na_2O$ of the fracture face heated at 850°C showed almost no pores whereas above 900°C many large pores were observed in the samples. At 850°C, plate shaped products of several ten nanometers in thickness were piled up and were interlocked with one another. This observed morphology was similar to that of fracture face of mica-based machinable glass-ceramics; which have been shown to have good machinability. SEM observations of the polished face showed presence of bright and dark portions due to the difference in the atomic number contrast of the formed phases. EDS analysis confirmed that the bright grains are a calcium phosphate phase, indicating the presence of β-CPP crystal. Although the presence of β-TCP crystal was not found in the photo, it was however confirmed by XRD. The amount of β-TCP crystal may have been relatively small and titanium was included in dark portions in the photo. [37]

3) Calcium phosphates containing Fluorine and Titania

The formation of fluoroapatite (FAP) was one of the ways to improve the chemical durability of calcium-phosphate glass-ceramics, as FAP has the lowest solubility among various calcium phosphate crystals. Kasuga et al (2007) [41] investigated a calcium phosphate glass-ceramic for a dental filler based on the composition: $40CaO\text{-}25TiO_2\text{-}30P2O_5\text{-}5CaF_2$ [CTP-F] (Ca/P = 0.67) and for a comparative study he also prepared a glass-ceramic without fluorine: $45CaO\text{-}25TiO_2\text{-}30P_2O_5$ [CTP]. He found that the glass-ceramic CTP-F had good chemical durability. He later prepared (2009) a calcium titanium phosphate glass-ceramic with improved chemical durability, more than observed in glass-ceramic CTP-F and this glass-ceramic was prepared by using the composition: $35CaO–10CaF_2–30P_2O_5–25TiO_2$ in mol % [CFPT] (Ca/P = 0.58) and again in this study he used CTP again for comparison. By using 10 mol % CaF_2

and restricting the Ca/P to 0.58 it was found that the chemical durability of the glass-ceramic CFPT was enhanced in comparison to glass-ceramic CTP-F. [42]

Kasuga's XRD analysis on calcium titanium phosphate glass-ceramic with and without fluorine, CTP-F and CTP respectively showed peaks assigned to Nasicon-type crystal: $CaTi_4(PO_4)_6$ and peaks assigned to $Ti(PO_3)_3$ and $(TiO)_2P_2O_7$ crystals. Once CaF_2 was added to the composition, apatite crystal was formed and CTP-F showed a weaker peak intensity of $CaTi_4(PO_4)_6$ crystal than in the CTP glass-ceramic. [41] A later study by Kasuga et al (2009) showed that the glass-ceramic CTP had crystalline phases such as α-$Ca_2P_2O_7$, $CaTi_4(PO_4)_6$, TiO_2 (anatase), and $(TiO)_2P_2O_7$, whilst CFPT contained only Ca-$Ti_4(PO_4)_6$ and apatite phases. The XRD peaks of CFPT glass–ceramic were sharp and their intensities were strong compared to the CTP glass-ceramic. [42]

DTA curves from Kasuga's study (2009) showed the glass transition temperatures, Tg of CTP and CFPT glasses to be 675°C and 615°C, respectively. The crystallisation temperatures were 785°C and 685°C of CTP and CFPT glasses respectively and the lower crystallization temperature was due to fluorine inclusion. [42] In most cases, the chemical durability of glasses and glass–ceramics is reduced when fluorine is added. However in Kasuga's study the crystallisation behaviour of the CTP glass was considerably influenced by adding a small amount of fluorine and the resulting glass–ceramic showed excellent chemical durability. [42]

SEM micrographs of CTP-F glass-ceramic surface showed small-sized pits which were believed to be initiated from the dissolution of crystalline and/or glassy calcium phosphate phases in the glass-ceramics. [41]

SEM images of CTP and CFPT glass–ceramics showed different morphologies. In the CPT glass–ceramic, the characteristic morphology was suggested to result from a spinodal-type phase separation of the glass before crystallisation was observed. [42] Earlier studies revealed that, in this sort of glass–ceramic, a calcium phosphate phase and a Nasicon-type crystalline phase such as $CaTi_4(PO_4)_6$ were three-dimensionally intertwined, and the calcium phosphate phase was easily dissolved and removed by acid treatment.[43-44] On the other hand, in the CFPT glass–ceramic several independent pits several tens of nanometers in size were observed just as in the previous study. The composition of the surface from EDS analysis was suggested to be the $CaTi_4(PO_4)_6$ phase and it was suggested that the apatite phase was leached out and was rooted in the $CaTi_4(PO_4)_6$ phase. [42]

During the heat treatment of CFPT glass, formation of apatite and $CaTi_4(PO_4)_6$ occurred. The apatite was several tens of nanometers in size and was embedded in the $CaTi_4(PO_4)_6$ phase. In the formation of the apatite and $CaTi_4(PO_4)_6$ phase, the orthophosphate group in the glass was consumed. And due to formation of these phases, there was a decrease in the amount of phosphate which resulted in the controlled formation of crystalline phases such as titanium phosphate and calcium pyrophosphate in the CTP glass–ceramic. It was suggested that preferential apatite formation was suggested to occur in glasses containing the orthophosphate group. [42]

Furthermore, EDS analysis demonstrated that in the glass-ceramic CFPT, fluorine was partially evaporated and 2.8% of residual fluorine was contained in the glass out of the 6% of fluorine initially used in the composition. [42]

Kasuga's Raman analysis demonstrated that the calcium phosphate glass-ceramics with and without fluorine, CTP and CTP-F respectively had peaks corresponding to

orthophosphate, pyrophosphate, and metaphosphate groups. The glass-ceramic containing fluorine (CTP-F) had sharper peaks than the CTP glass-ceramic which implied that there was a larger amount of crystalline phases in CTP-F than there was in the CTP glass-ceramic. Furthermore, the CTP-F glass-ceramic had larger intensities of peaks that correspond to the orthophosphate group than CTP. Generally the intensities of the peaks observed due to pyrophosphate group in both the spectrums were very small. In the CTP-F glass-ceramic, the peak corresponding to anatase was observed as supported by XRD. In the CTP glass-ceramic spectrum, a shoulder peak around 900cm^{-1} due to Ti-O_{nb} group (O_{nb}; non-bridging oxygen), was observed which is often seen in the glassy phase. It was thought that even after crystallisation, a fairly large amount of titanium constituent was included in the glassy phase. [41] In his later study (2009), it was shown that both CTP and CFPT glasses showed peaks corresponding to the orthophosphate group (PO_4^{3-}), the pyrophosphate group ($P_2O_7^{4-}$ group), and the metaphosphate group (PO_3^- group), which was in accord with Kasuga's earlier study of 2007. [41-42]

Furthermore, it was confirmed from the ^{19}F MAS-NMR spectra of CFPT, that the apatite in the glass–ceramic was a fluorine-containing oxyapatite, $Ca_{10}(PO_4)_6(O, F_2)$. [42]

Kasuga et al (2007) [41] found that the glass-ceramic, CTP-F had good chemical durability which was suggested to initiate from an increase in the amount of crystalline phases and a high content of titanium constituent in the residual glassy phase. It was observed that the incorporation of fluorine to the glass induced apatite formation in the glass and the apatite phase was an oxyapatite crystal containing fluorine. (fluoro-oxyaptite). [41] He later prepared a novel CFPT glass-ceramic which showed even more improved chemical durability than CTP-F. [42] It was shown that

the structure of the glass–ceramic was very much influenced by a small amount of fluorine included in the calcium phosphate glass. Fluorine-containing oxyapatite, $Ca_{10}(PO_4)_6(O, F_2)$ and Nasicon type, $CaTi_4(PO_4)_6$ phases were preferentially formed during heat treatment and apatite particles several tens of nanometers in size were fixed in the Nasicon-type phase. Titanium ions were also included in the residual phosphate glassy phase. The microstructure of this glass-ceramic was suggested to result in the excellent chemical durability and this is shown to be promising results in order to design novel dental fillers. [42]

1.3 Benefits of Titania Addition to Calcium Phosphate Glasses

A lot of interest has been shown on the role of titania in calcium phosphate glasses. The titania content serves as an effective bulk nucleating agent in calcium phosphate glass (TiO_2 above 4 wt %). [45] Studies have confirmed that when TiO_2 is added to calcium phosphate glasses, it improves its glass-forming ability, it improves the chemical durability of the glass, [26, 46] its modulus of elasticity, [26] it raises the glass viscosity, which was shown by an increase in the glass-transition temperature, Tg and consequently strengthens the glass network. [45, 47] Furthermore, studies have shown that when TiO_2 is added into calcium phosphate glasses, it increases the bulk density of the glass, [47] Moreover, it has been shown by Brauer et al (2007) [48] in the glass composition: P_2O_5-CaO-MgO-Na_2O-TiO_2 (whereby the glasses ranged from ultra and polyphosphate glasses to pyrophosphate glasses) that the incorporation of TiO_2 into calcium phosphate glasses not only decreases the solubility of the glasses but it also decreases the crystallization tendency by forming cross links between TiO_4 or TiO_6 structural groups and phosphate tetrahedra. [48]

A study by Neel at al (2008) [47] reported the effect of increasing titania on calcium phosphate glasses based on the general composition: CaO-P_2O_5-Na_2O. Glasses of 15

mol % TiO_2 were successfully produced however, glasses with 20 mol % could not be produced as they crystallised easily during cooling. By incorporating 15 mol % TiO_2 into the glasses, the bulk density increased which was due to the replacement of the low-density element Na^+ with the high-density element Ti^{4+}. Analysis of DSC data showed that the addition of TiO_2 resulted in a significant increase in Tg values. DTA results showed that the glass containing 5 mol % TiO_2 showed two crystallisation peaks, however the glass-free TiO_2, and the glasses containing 10 and 15 mol % TiO_2 showed only one crystallisation peak. Addition of 10 and 15 mol % TiO_2 produced glass structures with two broad melting peaks ranging instead of a single sharp melting peak as seen for the ternary glass with no TiO_2. [47]

Ternary glass with no TiO_2 produced a $NaCa(PO_3)_3$ phase which was identified from XRD. Glasses with 5 mol % TiO_2, produced two phases: $NaCa(PO_3)_3$ was the main phase, and TiP_2O_7 was the secondary phase. The glass with 10 and 15 mol % TiO_2, produced another phase, β-CaP_2O_6. For glass containing 15 mol % TiO_2, TiP_2O_7 became the main phase, instead of $NaCa(PO_3)_3$ which was the main phase for all other compositions. [47]

The glasses containing TiO_2 (5, 10 and 15 mol %) showed a reduction of one order of magnitude in degradation rate compared to TiO_2 free glass which suggested that addition of TiO_2 beyond 5 mol % does not produce further significant reduction in the degradation rate compared to 5 mol % TiO_2 containing glasses. Hence it can be proposed that there is an optimal amount of Ti^{4+} ions to be incorporated into the glass network to reduce the degradation, beyond which addition of more Ti^{4+} ions has no effect on degradation rate. [47]

Furthermore, addition of titania to calcium phosphate glasses has shown to induce formation of β-CPP and β-TCP during heat treatment [36] and is known to produce a calcium phosphate phase (apatite layer) on the surface of the glass-ceramic and hence has shown bioactivity. Addition of titania has shown to improve chemical durability of glasses and it is thought that the apatite formation is influenced by the durability of the glassy phase in the glass-ceramics. Apart from this, the glass-ceramic containing titania has shown relatively high fracture toughness, K_{IC} (1.9 MPa $^{m0.5}$) and bending strength (100-120 MPa). The toughness has been shown to be approximately twice larger than that of TCP or HA ceramics. [49] The glass-ceramic containing titania has enhanced mechanical properties as well as toughness, which is promising as a novel glass-ceramic with bioactivity for biomedical applications. [33]

1.4 Benefits of Fluorine Addition to Calcium Phosphate Glasses

The addition of fluorine to calcium phosphate glasses has shown to produce a fluoroapatite phase upon crystallisation. Fluoroapatite is known to be the least soluble amongst various calcium phosphate crystals such as hydroxyapatite and hence due to its least solubility characteristic, it improves the chemical durability of the glass-ceramic. Studies have shown that addition of fluorine to glasses results in excellent durability of the glass. [41-42] Furthermore, the amount of fluorine in a glass has an influence on its crystallisation behaviour, and can influence both the crystallisation mechanism and the phases formed. Fluorine is a network modifier and hence rearranges the glass network which causes crystallisation of the glass to occur more readily. It also decreases the refractive index of the glass and hence disrupts the glass network, facilitating glass degradation. Fluorine also reduces the melting temperature and glass transition temperature and as a network modifier it forms non bridging fluorines replacing non bridging oxygens. The glass network opens up and open up (disrupted) glass networks exhibit lower glass transition temperatures.

Calcium phosphate glasses containing fluorine have been used for many years. For example, in order to form glass ionomer cements, calcium fluoro-alumino-silicate glasses are commonly used for medical and dental applications. These types of glasses form apatite-mullite glass-ceramics by having the ability to crystallise into an apatite and mullite phase. Previous research by Freeman et al [58] has shown that this type of glasses have shown to have excellent osteoconduction and osteointegration properties when implanted in the body.

The structural role of fluorine in ionomer glasses has been studied extensively. Griffin and Hill [59] have researched the influence of fluorine on the glass properties for glasses based on the generic composition $4.5SiO_2$-$3.0Al_2O_3$-$1.5P_2O_5$-(5.0-x)CaO-$xCaF_2$ with x varying from 1 to 3.0. Their results showed that a decrease of 200^oC in the glass transition temperature can be observed when fluorine was introduced to the glass structure. This was expected as fluorine reduces the glass-network conductivity by replacing the bridging oxygens with non-bridging fluorines and therefore at a lower temperature the network relaxes.

A clear understanding of the mechanism by which the glass properties can be affected can be shown by a study of the coordination environment of fluorine in the glass network. Based on the composition $2SiO_2$-Al_2O_3-2(1-X)CaO-$XCaF_2$, Hill and Wood [60] studied a series of fluoro-alumino-silicate glasses and reported, that fluorine is bonded to aluminium atoms instead of silicon atoms. However earlier studies based on the composition $xSiO_2$-yAl_2O_3-$zCaF_2$ by Wilson et al. [61-62] suggested, that fluorine formed Si-F and Al-F bonds in SiO_3F and AlO_3F tetrahedra, respectively and thus it was suggested, that fluorine disrupted the glass network by substituting bridging oxygens with non-bridging fluorines as fluoride cannot bridge SiO_4

tetrahedra. Furthermore, numerous fractions of Al-O bonds were replaced by weaker non-network Al-F bonds which were confirmed by Zeng et. al. [63] who also suggested that the formation of non network Si-F bonds can be significant in aluminosilicate glasses. It is possible, that the formation of Si-F bonds is connected with the glass composition in addition to the fluorine content. Stebbins and Zeng [64] found evidence for the presence of Al-F-Ca(n) and F-Ca(n) species in the glass network, where n represents the number of Ca next nearest neighbouring fluorine in a $2SiO_2$-$2Al_2O_3$-$0.5CaO$-$0.5CaF_2$ glass.

Fluorine loss in calcium phosphate glasses has been a long standing issue. A lot of research has been conducted on fluorine loss in silicate glasses and it is known that fluorine is lost in the form of SiF_4 in these types of glasses. [65-66]

1.5 Aims and Objectives

The present research is based on calcium phosphate glasses with the composition: A. $1CaO$-$2P_2O_5$-$(1-x)CaF_2$-$xTiO_2$ (x = 0, 0.2, 0.6 and 0.8) where the Ca/P ratio was reduced to ≤ 0.5 as TiO_2 was added and B. $1CaO$-$2P_2O_5$-$1CaF_2$-$xTiO_2$ (x = 0.2, 0.5, 0.8 and 1) where Ca/P ratio remained constant at 0.5 as TiO_2 was added. An early realisation demonstrated that a glass having a Ca/P of > 0.5 could not be made and fluorine was not retained in the structure. The aim of this research was to make a fluorine containing calcium phosphate glass with a Ca/P of 0.5 and less, in the hope to retain fluorine by the addition of TiO_2 and investigate the effect of TiO_2 on the structure and crystallisation of the glasses.

CHAPTER 2

2. Materials and Methods

2.1 Materials

2.1.1 Preparation of Type A glasses

Table 2.1: Composition of type A glasses, TiO_2 addition for CaF_2 ($Ca/P \leq 0.5$)

Glass code	CaO	P_2O_5	CaF_2	TiO_2	CaF_2 (%)	TiO_2 (%)
CP	2	2	0	0	25	0
$CPFTR_2$	1	2	0.8	0.2	20	5
$CPFTR_3$	1	2	0.4	0.6	10	15
$CPFTR_4$	1	2	0.2	0.8	5	20

All the components above were weighed out in order to get approximately 100g of glass for each composition. Calcium carbonate ($CaCO_3$) was used to provide calcium oxide (CaO) in the glass. The powders were mixed by hand for approximately 45 minutes and the resulting mixture was transferred into a platinum crucible which was then placed in an electric furnace at a temperature of 1200°C for 1 hour. Then the crucible was taken out the furnace and the glass was quenched on a clean steel plate. After quenching, the glass frit formed was stored in a desiccator. The glass $CPFTR_4$ was not produced as the mixture crystallised in the platinum crucible during melting.

2.1.2 Preparation of Type B glasses

Table 2.2: Composition of type B glasses, TiO_2 addition ($Ca/P = 0.5$)

Glass code	CaO	P_2O_5	CaF_2	TiO_2	CaF_2 (%)	TiO_2 (%)
CPCTA	1	2	1	0.2	23.8	4.76
$CPCTA_2$	1	2	1	0.5	22.2	11.11
$CPCTA_3$	1	2	1	0.8	20.8	16.66
$CPCTA_4$	1	2	1	1	20	20

The preparation of the above glasses was the same as the one described for the glasses in paragraph 2.1.1.

2.2 Methods

2.2.1 Crystallisation of Glasses

A heat-treatment route was followed for the crystallisation of glasses starting at 100°C up to Tp+50°C above the crystallisation temperature of each of the samples. The heating rate was 8°C/min and when the furnace reached the desired temperature the glass was held to be crystallised for one hour. Afterwards, the temperature was decreased to room temperature at a rate of 8°C/min. To ensure the glasses would not stick to the crucible and for the glass-ceramic to be taken out with ease, the samples were placed in an alumina crucible with a platinum foil.

2.2.2 Cold Mounting of Glass-ceramic Samples for Microscopy

In order to prepare for ESEM samples, cold mounting of glasses was carried out. An epoxy resin and hardener (EPOFIX supplied by STRUERS, UK) was used and mixed together at a ratio of 15 parts of resin per volume to 2 parts of hardener per volume. The mixing was done for 2 minutes in such a way to have as fewer air bubbles as possible. After that the mixture was left to rest for 2 minutes and then it was poured into a mould where the sample was placed. This was then left to set overnight.

2.2.3 Polishing of Glass-ceramic Samples for Microscopy

For the progressive polishing of the samples both a DAP-7 and Pedemin-S polishing machine were used as well as a series of polishing discs. Specifically; Struers MD-Piano, MD-Largo, MD-Chem and MD-Dac. Three samples were placed in the polishing machine each time and the first polishing disc to be used was the MD-Piano. Water was used as a lubricant for the use of MD-Piano and this disc was used until the sample was plane. MD-Piano was used with about 5-15 N and it lasted about 40 minutes. In order to maintain a constant removal of material, MD-Piano was dressed at regular intervals by placing the dressing stick in the centre of the rotating

MD-Piano disc and moved towards the edge using only a modest force. This was done when the water was switched on so to lubricate and flush the materials removed from the surface. After the polishing of MD-Piano was complete, MD-Largo was used with a liquid diamond suspension and a particle size of 9μm. The load for MD-Largo was about 5-15 N and it lasted almost 20 min. Then, MD-Dac was used with a load of 5-15 N and the lubricant used was a liquid diamond suspension with a particle size of 3μm. The duration of the polishing with MD-Dac was about 10 min. Finally, MD-Chem was once again used with a load of 5-15 N with a liquid diamond suspension and a particle size of 0.04μm and lasted approximately 5 minutes. The respective diamond suspensions were used to obtain a smooth surface of the glass-ceramic in order for SEM-EDX measurements to be performed.

2.2.4 Fourier Transform Infra-Red Spectroscopy (FTIR)

The FTIR powder absorption spectra were recorded using a Nicolet 860 Magna spectrometer, in the 4000-400 nm region with a resolution of 4 cm^{-1} and the number of scans was 100 per minute. Both the FTIR data for type A and B glass and glass-ceramics were measured at room temperature. In order to obtain the spectra, a KBr pellet was used with approx. 0.5 wt% of sample concentration. The KBr method was used in order to increase the resolution of the spectra obtained. The background using a control sample of KBr was always taken prior to each measurement.

2.2.5 Differential Scanning Calorimetry (DSC)

Differential scanning calorimetry (DSC) was used to examine the thermal transitions of the glass compositions including glass transition temperature, crystallisation temperature and melting temperature. The instrument used was a NETZSCH 404C DSC and the DSC analysis was performed within a temperature region from 100°C to 1200°C at a heating rate of 10°C/min. The analysis was performed using Argon gas,

in order to achieve a controlled heat flow and protect the furnace from the high temperature used. The preparation of DSC samples involved using a pestle and mortar in order to grind the samples into a powder of fine particles; the size of the particles was <100µm. Two platinum pans were used, the empty one being the reference pan and the one with the glass sample being the sample pan. The crystallization temperature (Tp) and the melting temperature (Tm) were both taken as the peak temperatures of the crystallization exotherm and the melting endotherm, respectively. An example of the calculation of glass transition temperature of glass CP containing 0 % TiO_2 is shown in figure 2.1 below. For all of the glasses, this method of calculation was used.

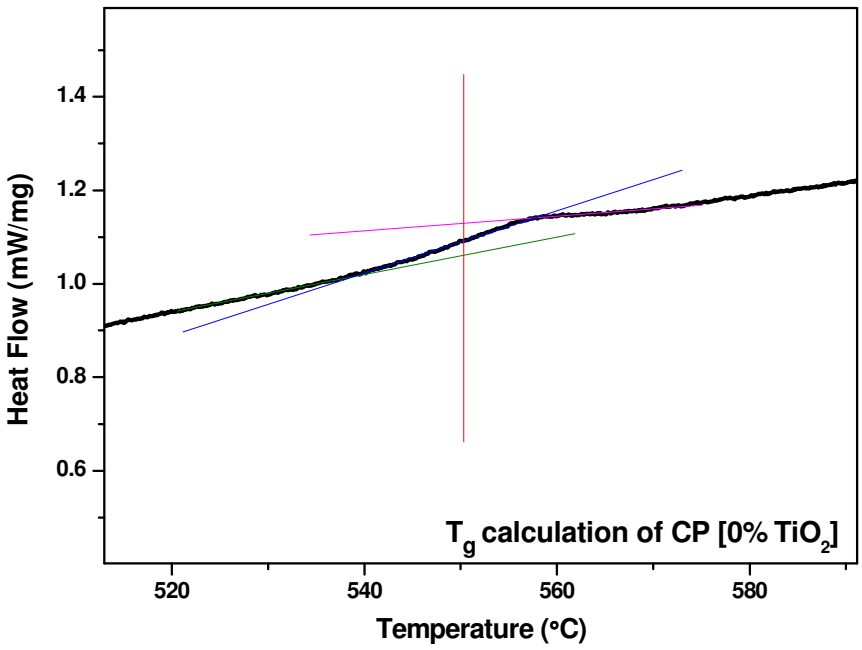

Figure 2.1: An example of the calculation of glass transition temperature of glass CP containing 0 % TiO_2

2.2.6 X-ray Diffraction (XRD)

The heat treated glass-ceramics as in 2.2.1 were used and were grounded into a powder. The XRD was conducted using a Panalytical X-Pert X-Ray powder diffractometer with a Cu anode, at 40 kV and 40 mA. The X-ray diffraction was

performed at continuous scan mode with values of 2θ between 0° and 80° and a step size of 2θ=0.0200°.

2.2.7 Thermogravimetric Analysis (TGA)

Thermogravimetric analysis was conducted on only the amorphous glasses to see whether any mass loss occurred during the making of the glasses. It was performed using NETZCH 449 STA with a temperature region from 50°C to 1250°C and a heating rate of 10 °C /min. The preparation for TGA samples involved using a pestle and mortar in order to grind the samples into a powder of particle size <100μm. Two platinum pans were used. One as a reference pan, which remained empty throughout the experiment and the other one, the sample pan, where the glass powder was placed in. The method used for determining mass loss was the mass loss of each of the glasses over the 50-1250°C range. Therefore the mass at 1250°C for each of the glasses was deducted from the initial mass at 50°C for each of the samples.

2.2.8 Environmental Scanning Electron Microscopy (ESEM)

Micrographs were obtained using an XL 30 ESEM FEG electron microscope operated at an acceleration voltage of 20 kV and using the SEM mode in order to investigate the microstructure of glass-ceramics. The analysis took place under conditions of high vacuum. Before the analysis took place, the samples were etched with hydrofluoric (HF) acid (7%). The samples were mounted onto a microscopy stab and they were coated with carbon. Silver paint was used from the edge of the coating till the surface of the stab so that the sample became conductive to reduce charging.

2.2.9 Energy Dispersive X-ray analysis (EDX)

Energy dispersive x-ray analysis is a method used for qualitative and sometimes quantitative analysis of the elements present in a material. EDX was therefore

utilized to gain further elemental information about the samples. EDX was conducted on the surface of the glass-ceramics and in order for the samples to be analysed, they were less than 2 μm in size for accuracy. The EDX analysis software settings were kept the same throughout the analysis of all samples and these were; Livetime seconds = 100, process time = 5, spectrum range (Kev) = 0-40, Number of channels = 2K and the deadtime was constantly checked to see if it was low (approximately 20-25 seconds) in order for samples to be analysed accurately. In order to see what crystal phases were present in the samples, I chose different parts of the sample to analyse in order to observe the different crystal morphologies.

2.2.10 Density Measurements

In order for the density of the phosphate glasses to be calculated the Archimedes principle was used. The glasses were weighed separately in air and ethanol. Then the density of the glasses was measured using the following equation:

$$\rho = (\textit{weight of glass in air} \times \textit{density of ethanol}) / (\textit{weight of dry glass} - \textit{weight of immersed glass}) \qquad \text{(Eq 2.1)}$$

Where: ρ = *Density*

Where the *density of ethanol* = *0.789 g/cm*^{3}

All measurements were conducted at room temperature. Subsequently, the oxygen density of the phosphate glasses was calculated using the following equation:

$$\rho_{oxygen} = (\rho_{glass} \times MW_{oxygen}) / MW_{glass} \qquad \text{(Eq 2.2)}$$

Where:

ρ_{oxygen} = *Oxygen Density*

ρ_{glass} = *Density of glass*

MW_{oxygen} = *Molecular weight of oxygen*

MW_{glass} = Molecular weight of glass

CHAPTER 3

3. Results

3.1 Glasses

The only glasses that could be made were CP, the glass which only contained calcium and phosphorus without TiO_2 or CaF_2. $CPFTR_2$ could also be made which used the addition of 5 mol % TiO_2 for the CaF_2. $CPFTR_3$, which used 15 mol % TiO_2 addition, crystallised easily upon cooling on the stainless steel plate and hence was not amorphous. Moreover, $CPFTR_4$ could not be made as the mixture did not flow as a melt and was crystallised in the crucible. (See table below.)

The table below summarises the glasses that could and could not be made with TiO_2 addition for CaF_2. (Ca/P = ≤0.5)

Table 3.1: Ability to form glasses with TiO_2 addition for CaF_2 (type A glasses)

Glass code	CaO	P_2O_5	CaF_2	TiO_2	TiO_2 (mol %)	CaF_2 (mol %)	Ability to form glass
CP	2	2	0	0	0	0	√ -amorphous
$CPFTR_2$	1	2	0.8	0.2	5	20	√ - amorphous
$CPFTR_3$	1	2	0.4	0.6	15	10	Crystallised upon cooling
$CPFTR_4$	1	2	0.2	0.8	20	5	X

In type B glasses, whereby TiO_2 was added with a constant Ca/P, the only glasses which could be made were CPCTA and $CPCTA_2$ whereby 4.76 mol % TiO_2 and 11.11 mol % TiO_2 were used respectively. $CPCTA_3$ and $CPCTA_4$ used 16.66 mol % and 20 mol % TiO_2 respectively and although both of them flowed as a melt, they both crystallised easily upon cooling.

The table below summarises the glasses that could and could not be made with TiO_2 addition. (Ca/P = 0.5)

Table 3.2: Ability to form glasses with TiO_2 addition (type B glasses)

Glass code	CaO	P_2O_5	CaF_2	TiO_2	TiO_2 (mol %)	CaF_2 (mol %)	Ability to form glass
CPCTA	1	2	1	0.2	4.76	23.8	√-amorphous
$CPCTA_2$	1	2	1	0.5	11.11	22.2	√-amorphous
$CPCTA_3$	1	2	1	0.8	16.66	20.8	Crystallised upon cooling
$CPCTA_4$	1	2	1	1	20	20	Crystallised upon cooling

It is worth noting, that the glass composition used in the making of glass CP was $2CaO2P_2O_5$ and therefore did not contain any TiO_2 or CaF_2. However, for the sake of comparison among our results the glass composition $1CaO2P_2O_51CaF_2$ was used for glass CP as they are both very similar glasses having the same calcium to phosphate ratio.

3.2 Differential Scanning Calorimetry Analysis of all Glasses

The glass transition temperature (Tg), the crystallization temperature (Tp) and the melting temperature (Tm) values for type A glasses are shown in Table 3.3, the main Tp and Tm values are presented in bold.

Table 3.3 DSC analysis of type A glasses; data run at 10°C/min

Glass code	TiO_2 (mol %)	CaF_2 (mol %)	Tg (°C)	Tp (°C)	Tm (°C)
CP	0	25	550	672	972
$CPFTR_2$	5	20	572	693, **770**	949, **976**
$CPFTR_3$	15	10	538	682	967

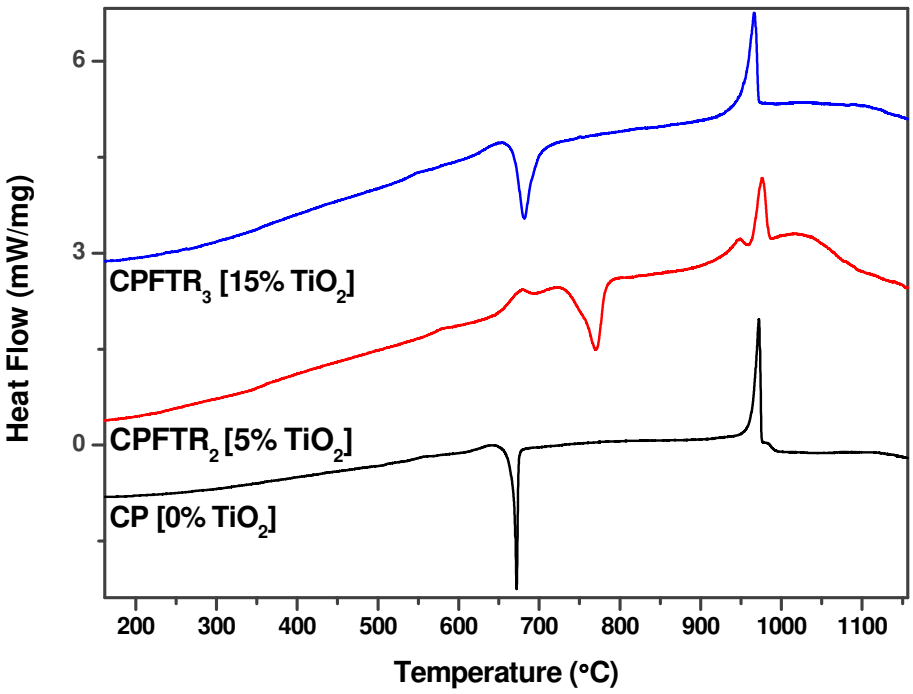

Figure 3.1: DSC of type A glasses

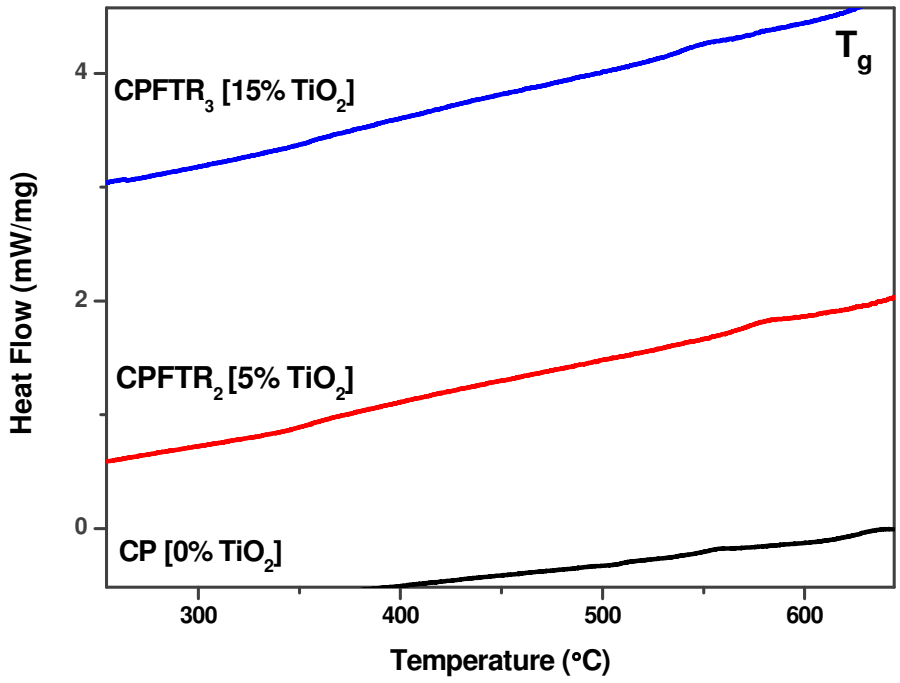

Figure 3.2: Glass transition temperature of type A glasses

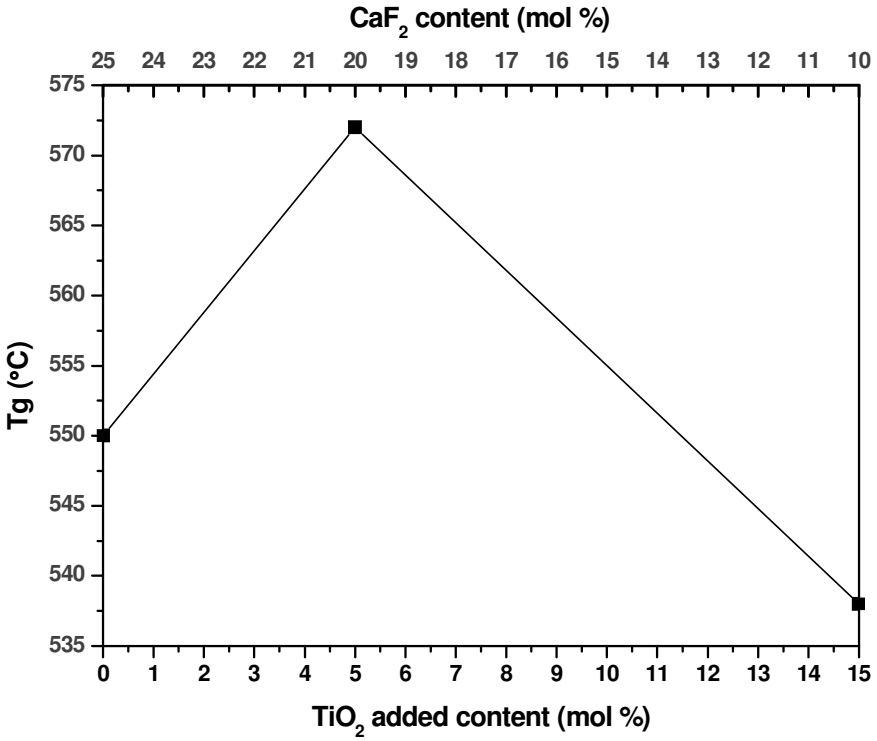

Figure 3.3: Change of glass transition temperature with TiO_2 added content for CaF_2 content in type A glasses.

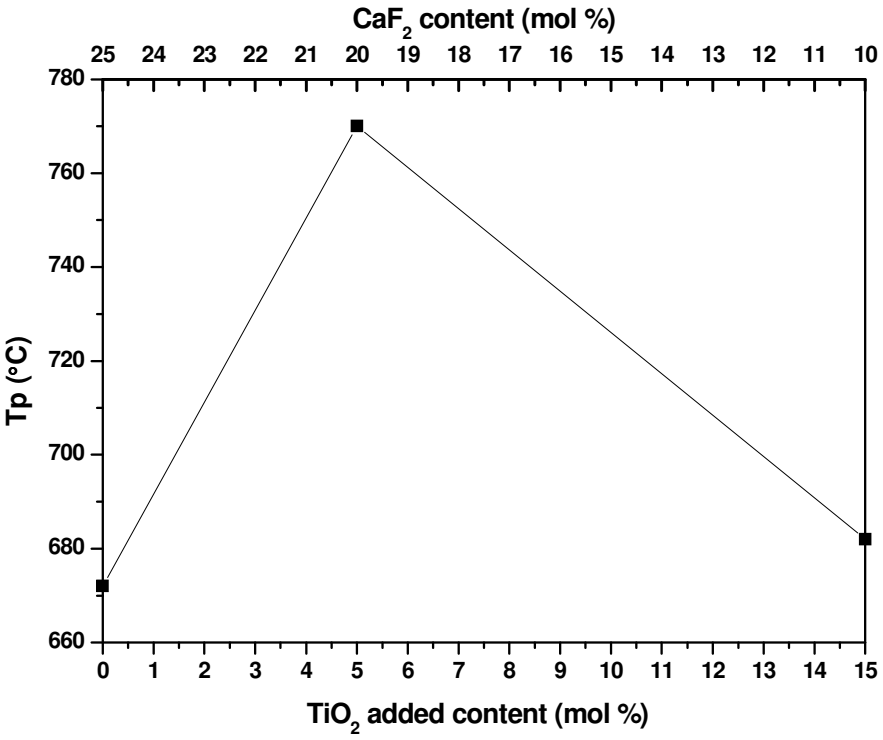

Figure 3.4: Change of main crystallization temperature with TiO_2 added content for CaF_2 content in type A glasses.

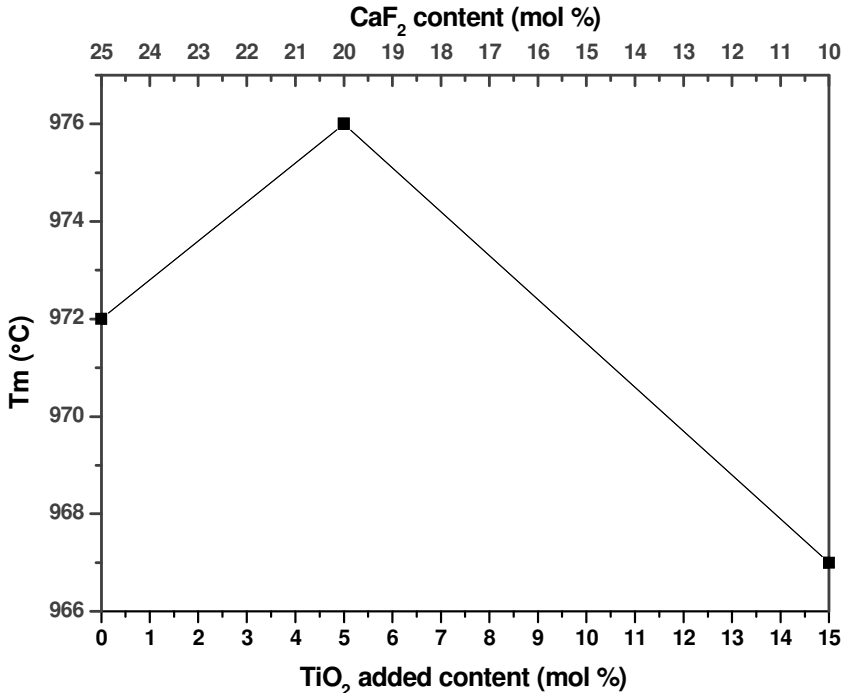

Figure 3.5: Change of main melting temperature with TiO_2 added content for CaF_2 content in type A glasses.

The glass transition temperature (Tg), the crystallization temperature (Tp) and the melting temperature (Tm) values for type B glasses are shown in Table 3.4.

Table 3.4: DSC analysis of type B glasses; data run at 10°C/min

Glass code	**TiO_2 (mol %)**	**CaF_2 (mol %)**	**Tg_1 (°C)**	**Tg_2 (°C)**	**Tp (°C)**	**Tm (°C)**
CPCTA	4.76	23.8	546	779	**698**, 725	**963**, 979
$CPCTA_2$	11.11	22.2	570	810	738, **777**	946, **975**
$CPCTA_3$	16.66	20.8	551	787	**720**	952, **978**
$CPCTA_4$	20	20	569	811	**751**	**974**

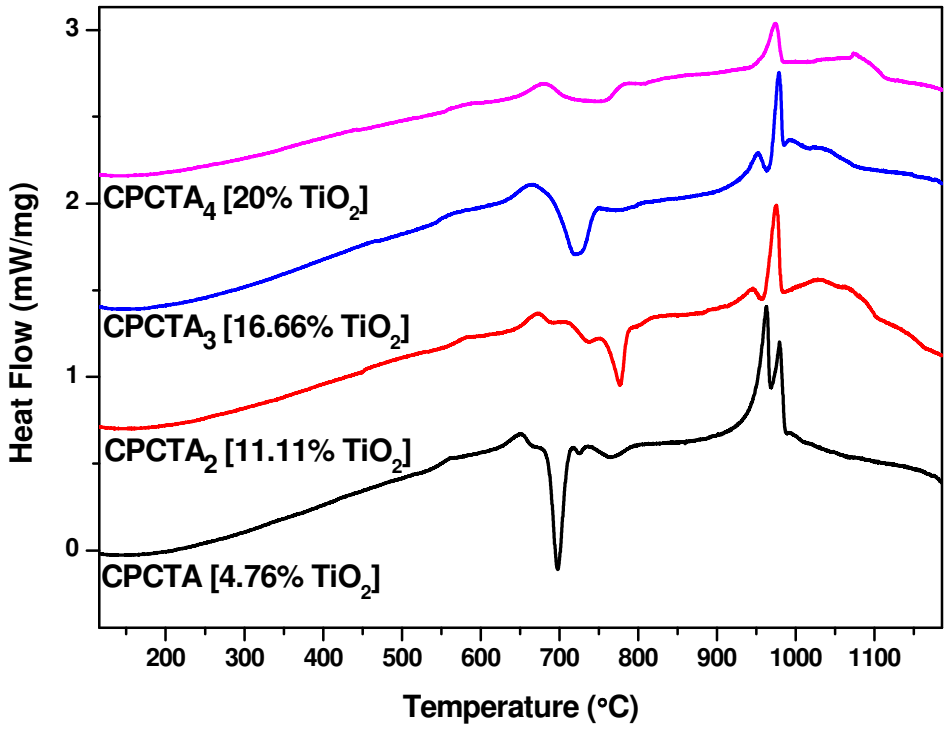

Figure 3.6: DSC of type B glasses

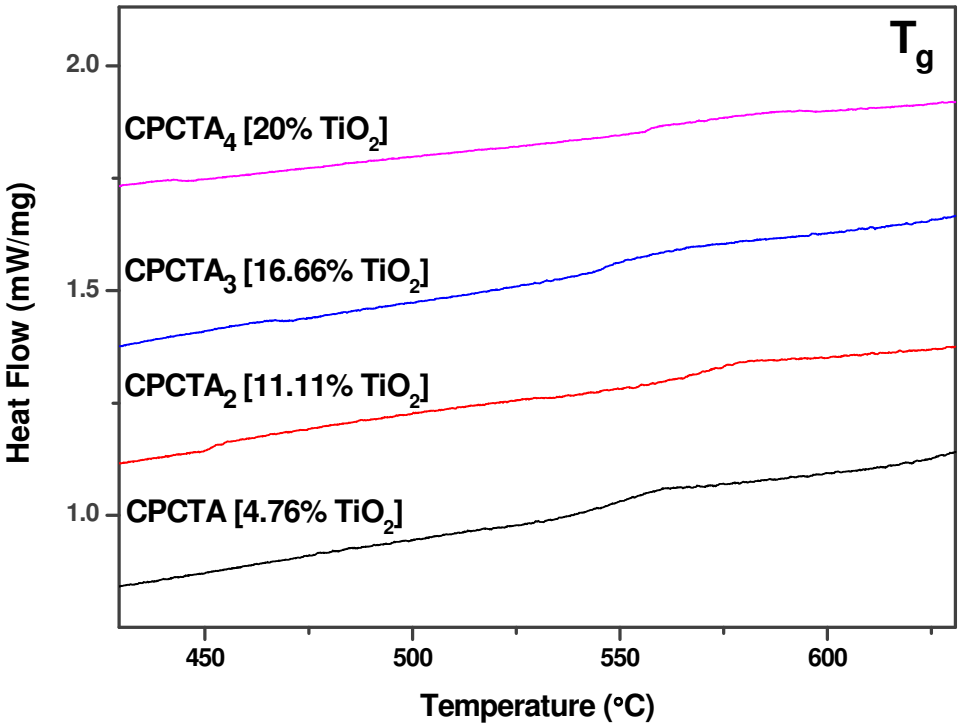

Figure 3.7: First glass transition temperature of type B glasses

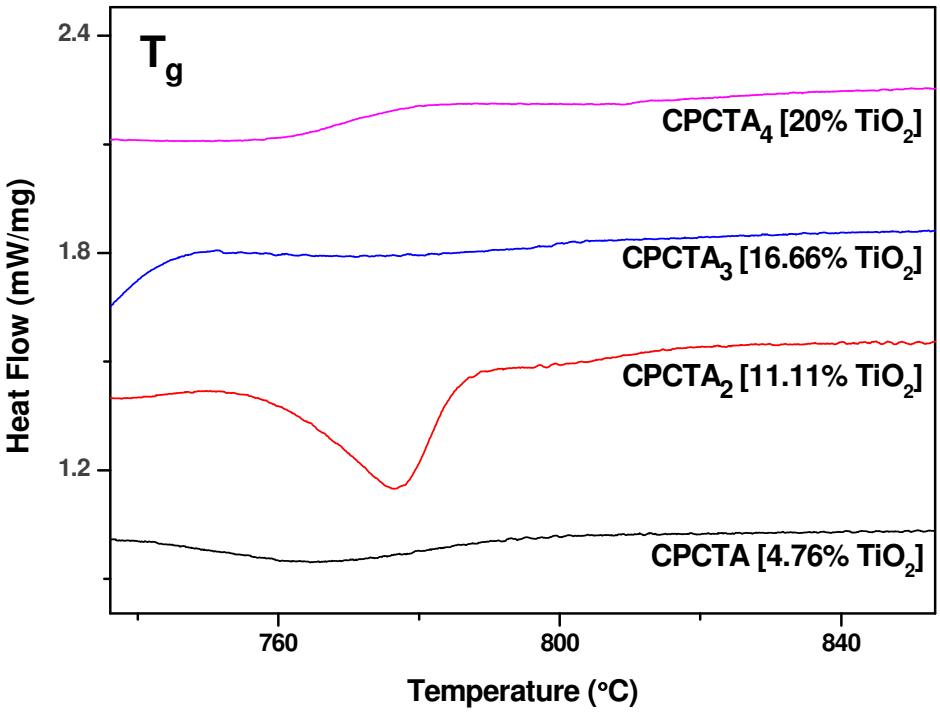

Figure 3.8: Second glass transition temperature of type B glasses

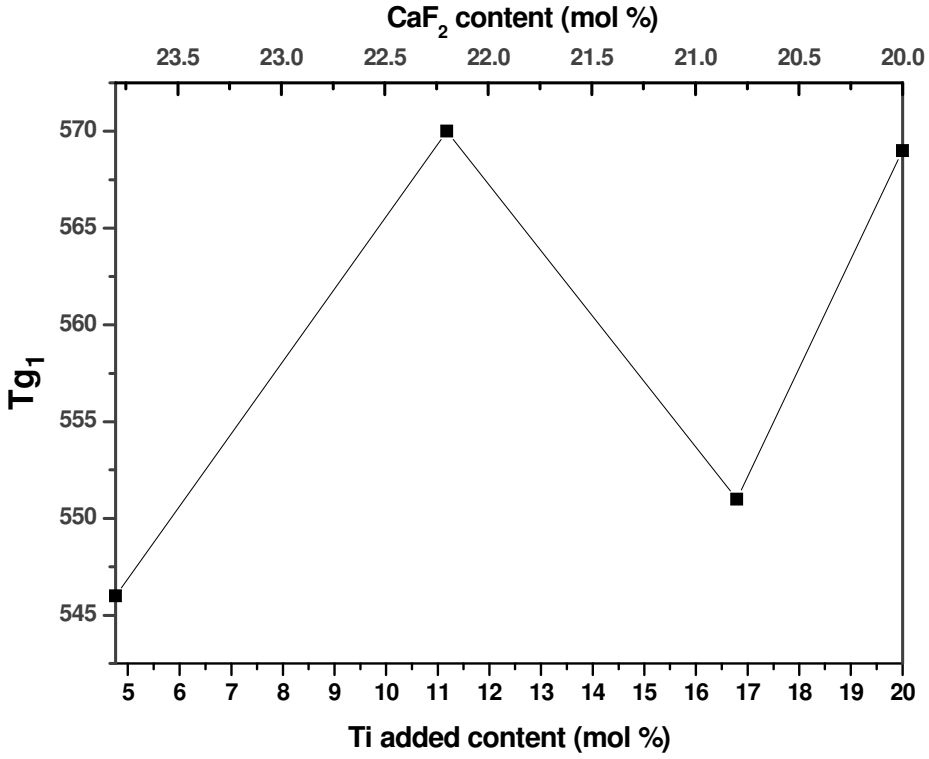

Figure 3.9: Change of first glass transition temperature with TiO_2 added content in type B glasses.

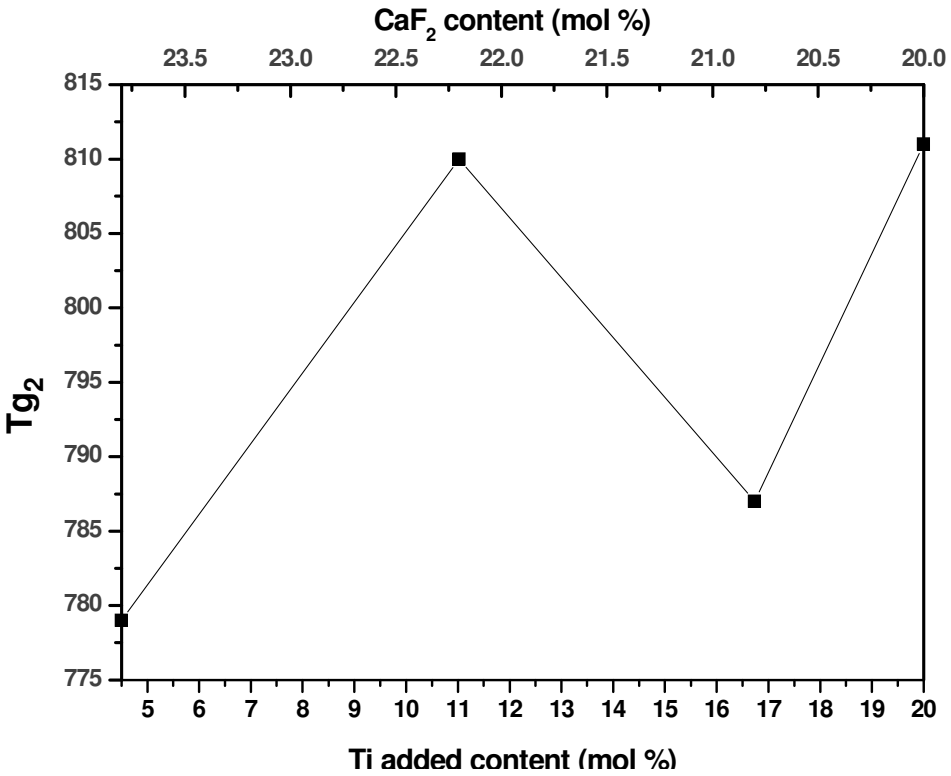

Figure 3.10: Change of second glass transition temperature with TiO_2 added content in type B glasses.

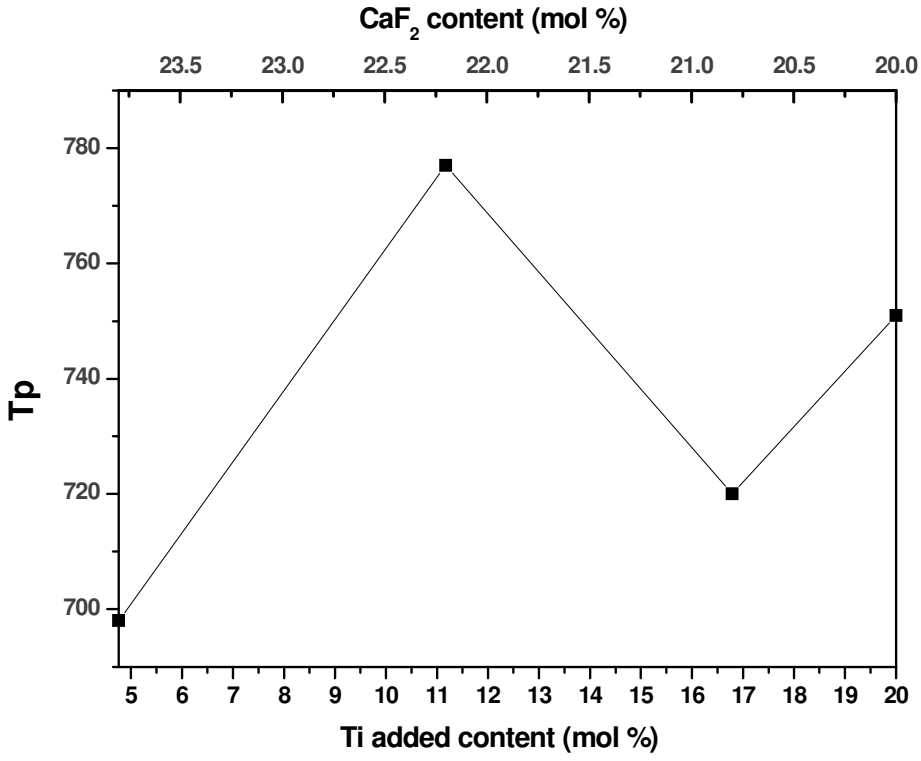

Figure 3.11: Change of main crystallization temperature with TiO_2 added content in type B glasses.

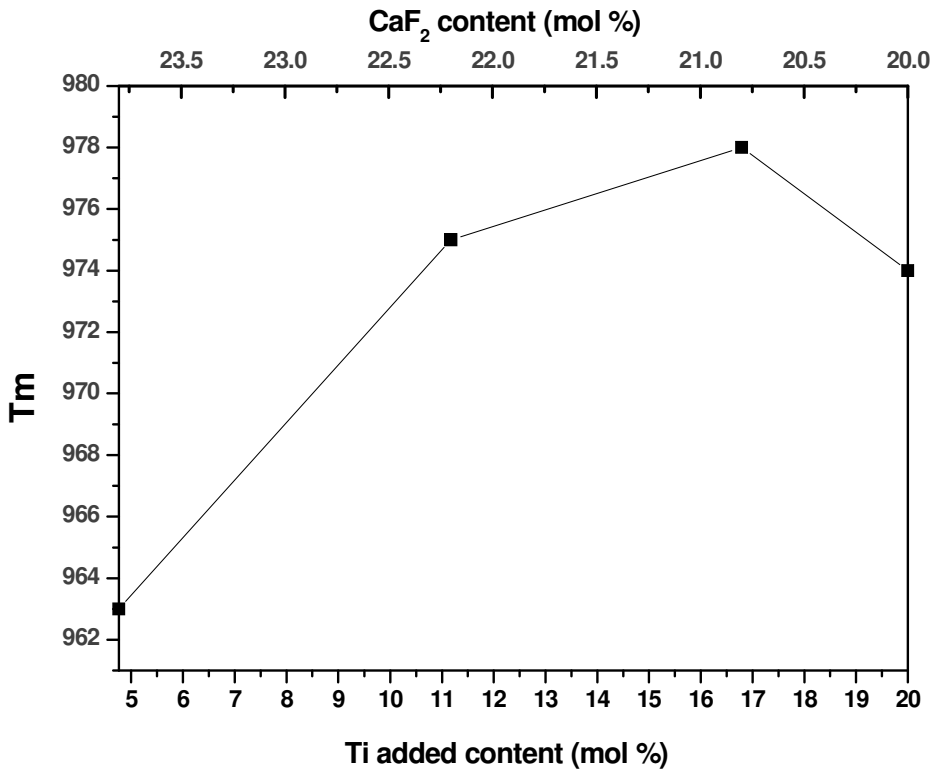

Figure 3.12: Change of main melting temperature with TiO_2 added content in type B glasses.

3.3 Density and Oxygen Density of all Glasses

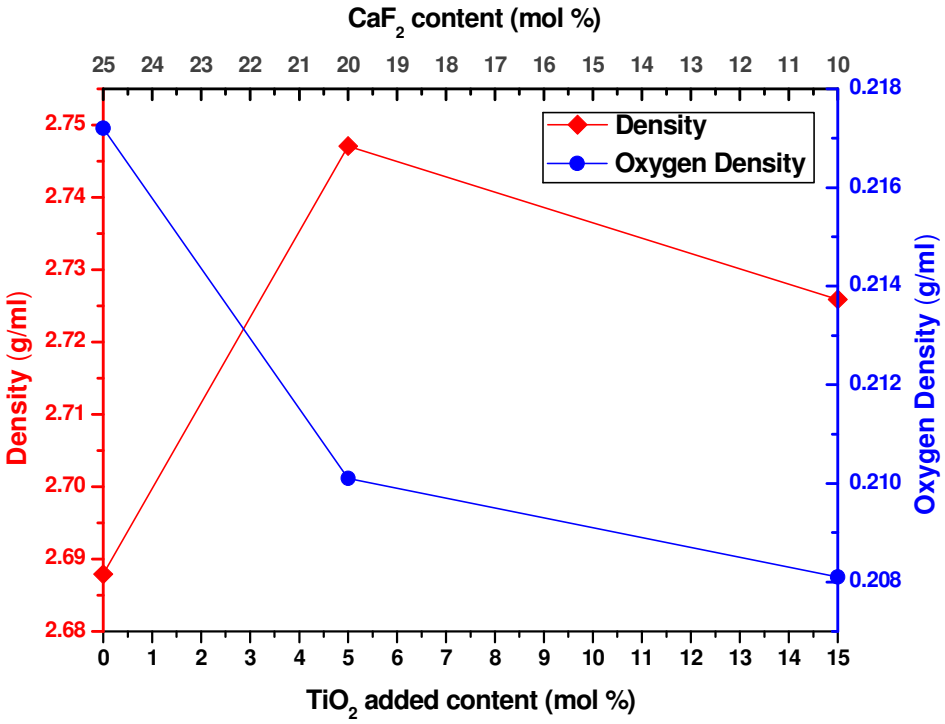

Figure 3.13: Density and oxygen density of type A glasses

Figure 3.13 shows the change in density and oxygen density in type A glasses with increased TiO_2 content. Note that the lines joining the data points in the above figure are only for visual reference as to plot them is indicative of knowledge of those intermediate values.

Table 3.5: Density and Oxygen Density of type A glasses

Glass code	TiO_2 (mol %)	CaF_2 (mol %)	Density ρ (g/cm^3)	Oxygen Density ρ_{oxygen} (g/cm^3)
CP	0	25	2.6879	0.2172
$CPFTR_2$	5	20	2.7471	0.2101
$CPFTR_3$	15	10	2.7259	0.2081

Table 3.5 shows the density and oxygen density values for type A glasses. The measured density values were parallel with the change in Tg for type A glasses. The calculated oxygen density values for type A glasses show a decrease which suggests that there is a change of the oxygen environment within the glass network.

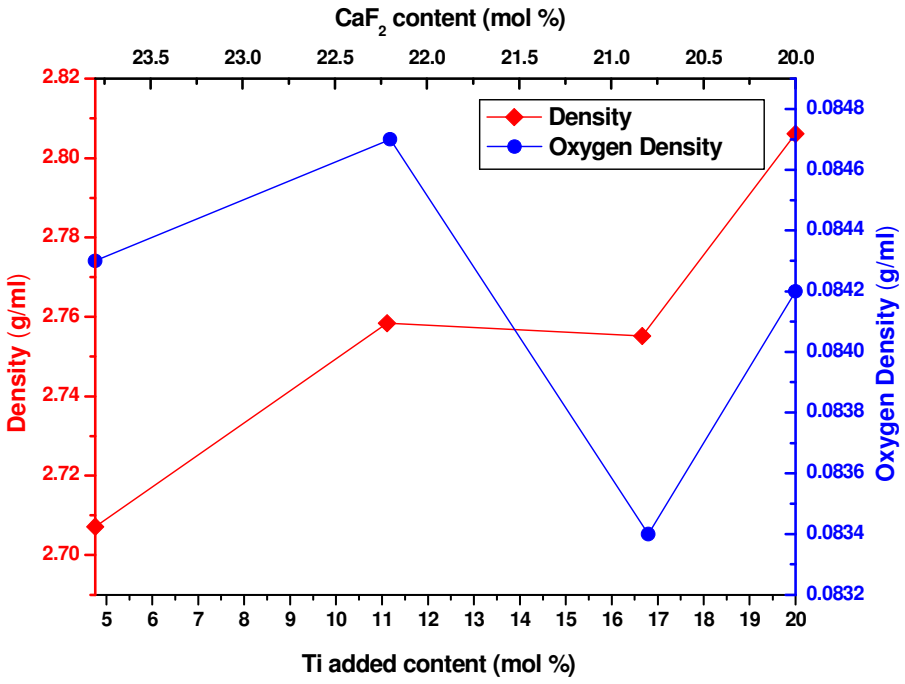

Figure 3.14: Density and oxygen density of type B glasses

Figure 3.14 shows the change in density and oxygen density in type B glasses with increased TiO_2 content. Note that the lines joining the data points in the above figure are only for visual reference as to plot them is indicative of knowledge of those intermediate values.

Table 3.6 Density and Oxygen Density of type B glasses

Glass code	TiO_2 (mol %)	CaF_2 (mol %)	Density ρ (g/cm^3)	Oxygen Density ρ_{oxygen} (g/cm^3)
CPCTA	4.76	23.8	2.7072	0.0843
$CPCTA_2$	11.11	22.2	2.7584	0.0847
$CPCTA_3$	16.66	20.8	2.7552	0.0834
$CPCTA_4$	20	20	2.8061	0.0842

Table 3.6 shows the density and oxygen density values for type B glasses. From the measured density values for type B glasses, it is indicative from these results that overall, the addition of TiO_2 into these calcium phosphate glasses where the Ca/P is kept constant at 0.5, causes the density of the glasses to be increased with the exception of glass $CPCTA_3$ which has shown to have a minute decrease in density and therefore is not significant. The calculated oxygen density values for type B glasses shows that there is a minor change in oxygen density when TiO_2 is added.

The density and oxygen density of type A and B glass-ceramics were to be measured using a helium pycnometer, in order to obtain accurate density and oxygen density values for the glass-ceramics. However due to time restrictions, they could not be measured. Although, it was expected the type A and B glass-ceramics would be denser than the type A and B glasses.

3.4 X-ray Diffraction Study of Glass-ceramics

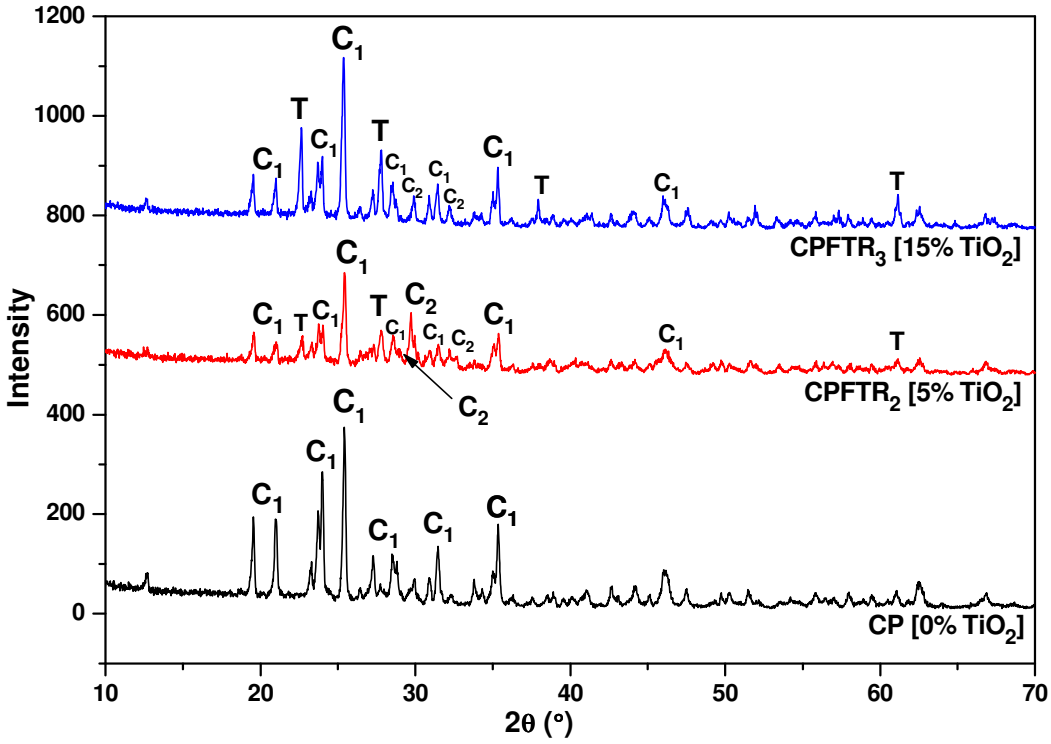

Figure 3.15: X-ray powder diffraction patterns of all type A glass-ceramics. C_1 = Calcium metaphosphate,, C_2 = Calcium pyrophosphate and T= Titanium pyrophosphate.

Table 3.7: Analysis of XRD spectra of type A glass-ceramics

Glass	TiO_2 (mol %)	CaF_2 (mol %)	Crystal phases		
CP	0	25	CaP_2O_6	x	x
CPFTR$_2$	5	20	CaP_2O_6	$Ca_2P_2O_7$	TiP_2O_7
CPFTR$_3$	15	10	CaP_2O_6	$Ca_2P_2O_7$	TiP_2O_7

The X-ray powder diffraction patterns of type A glass-ceramics with the calcium phosphate reference glass-ceramic are shown in Figure 3.15. Table 3.7 summarises the crystal phases present in type A glass-ceramics.

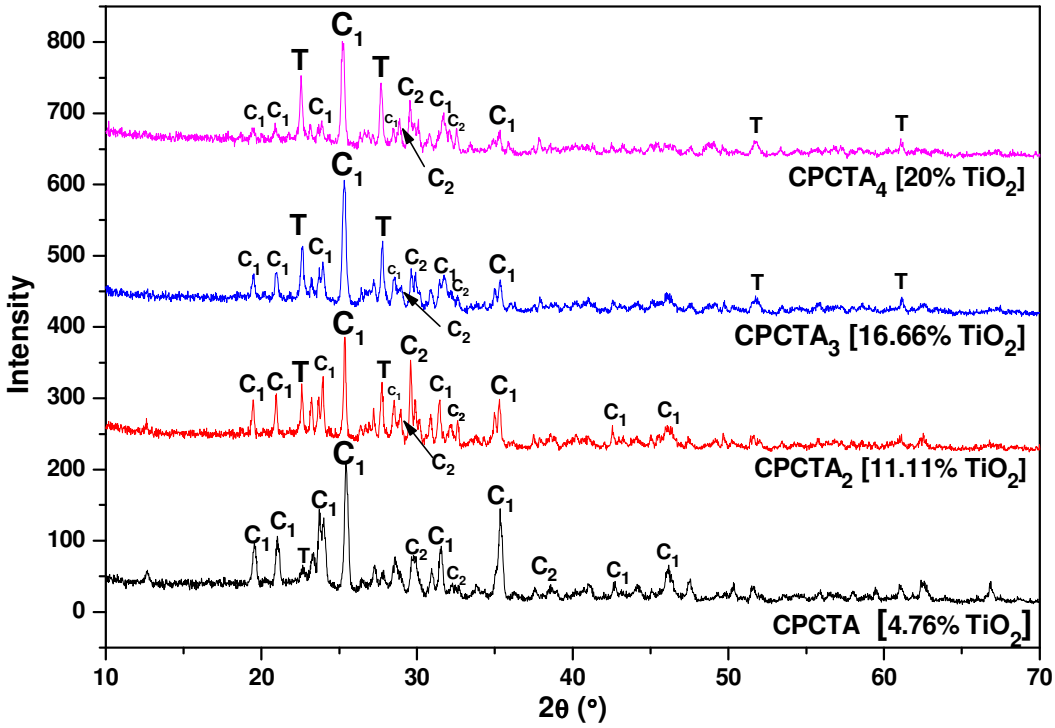

Figure 3.16: X-ray powder diffraction patterns of type B glass-ceramics. C_1 = Calcium metaphosphate, C_2 = Calcium pyrophosphate and T= Titanium pyrophosphate.

Table 3.8: Analysis of XRD spectra of type B glass-ceramics

Glass	TiO_2 (mol %)	CaF_2 (mol %)	Crystal phases		
CPCTA	4.76	23.8	CaP_2O_6	$Ca_2P_2O_7$	TiP_2O_7
$CPCTA_2$	11.11	22.2	CaP_2O_6	$Ca_2P_2O_7$	TiP_2O_7
$CPCTA_3$	16.66	20.8	CaP_2O_6	$Ca_2P_2O_7$	TiP_2O_7
$CPCTA_4$	20	20	CaP_2O_6	$Ca_2P_2O_7$	TiP_2O_7

The X-ray powder diffraction patterns of type B glass-ceramics are shown in Figure 3.16. Table 3.8 summarises the crystal phases present in type B glass-ceramics.

Overall, all the glasses are crystallised into a metaphosphate phase (CaP_2O_6) and upon TiO_2 addition in type A and in type B glasses, new crystalline phases such as $Ca_2P_2O_7$ and TiP_2O_7 emerge.

3.5 Fourier Transform Infrared Spectroscopy Study of Glasses and Glass-ceramics

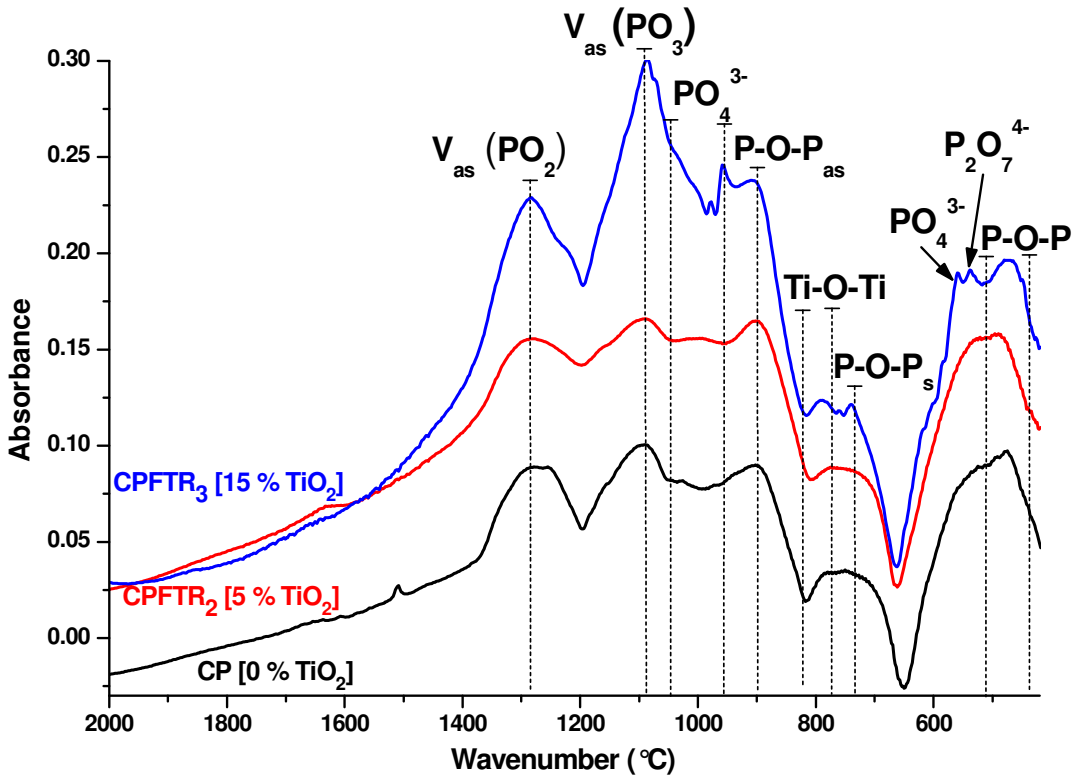

Figure 3.17: FTIR spectra of type A glasses

The FTIR absorption spectra of type A glasses is shown in Figure 3.17 measured at room temperature. Table 3.9 gives further description of FTIR spectra of type A glasses.

Table 3.9: Description of FTIR spectra for type A glasses.

Wavenumber (cm^{-1})	CP [0 % TiO_2, 25 % CaF_2]	$CPFTR_2$ [5 % TiO_2, 20 % CaF_2]	$CPFTR_3$ [15 % TiO_2, 10 % CaF_2]	Description
	1508	Shoulder at ~1620	-	OH-bending vibrations [50-51]
	1255	1281	1285	Asymmetric stretching vibration of PO_2 [50]
	1090	1090	1085	Asymmetric stretching vibration of PO_3^{2-} [52-54]
	1026	993	960-978	Symmetric stretching vibration of PO_4^{3-} [35]
	903	903	908	Asymmetric vibration of P-O-P linkages [53]
	-	-	760-790	Symmetric stretching vibration of Ti–O–Ti linkages in TiO_4 units. [55]
	750	750	745	Symmetric stretching vibration of P-O-P bridges [52]
	-	-	560	PO_4^{3-} bending vibrations [56]
	-	-	535	$P_2O_7^{4-}$ [50]
	474	496	480	P-O-P bending vibrations [50-53]

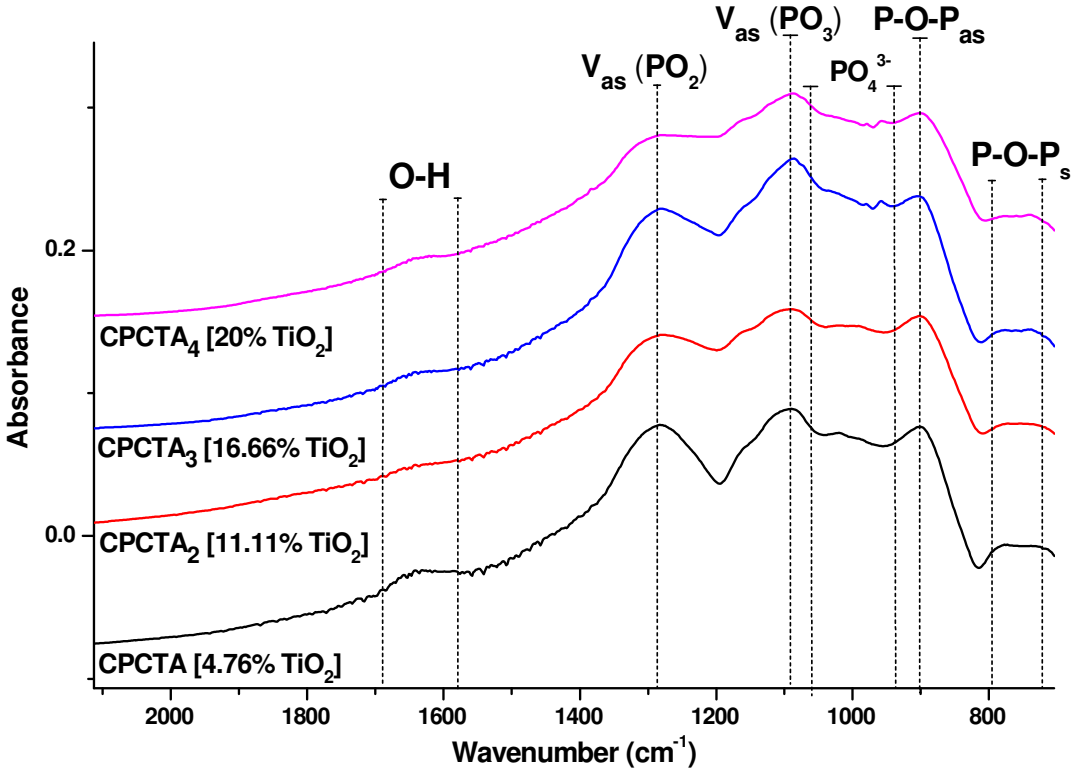

Figure 3.18: FTIR spectra of type B glasses

The FTIR absorption spectra of type B glasses are shown in Figure 3.18 measured at room temperature. Table 3.10 gives further description of FTIR spectra of type A glasses.

Table 3.10: Description of FTIR spectra for type B glasses

	CPCTA [4.76 % TiO_2, 23.8% CaF_2]	**$CPCTA_2$** [11.11 % TiO_2, 22.2% CaF_2]	**$CPCTA_3$** [16.66 % TiO_2, 20.8% CaF_2]	**$CPCTA_4$** [20 % TiO_2, 20 % CaF_2]	**Description**
Wavenumber (cm^{-1})	1560-1632	1560-1644	1565-1637	1600-1631	OH bending vibrations [50-51]
	1282	1275	1282	1282	Asymmetric stretching vibration of PO_2 from metaphosphate chains [50]
	1091	1090	1087	1084	Asymmetric stretching vibration of PO_3 [52-54]
	1021	1020	962-981	961	Symmetric stretching vibration of PO_4^{3-} [35]
	901	901	904	903	P-O-P asymmetric vibrations [53]
	725-773	735-773	735-778	735-775	Symmetric stretching vibration of P-O-P bridges [52]

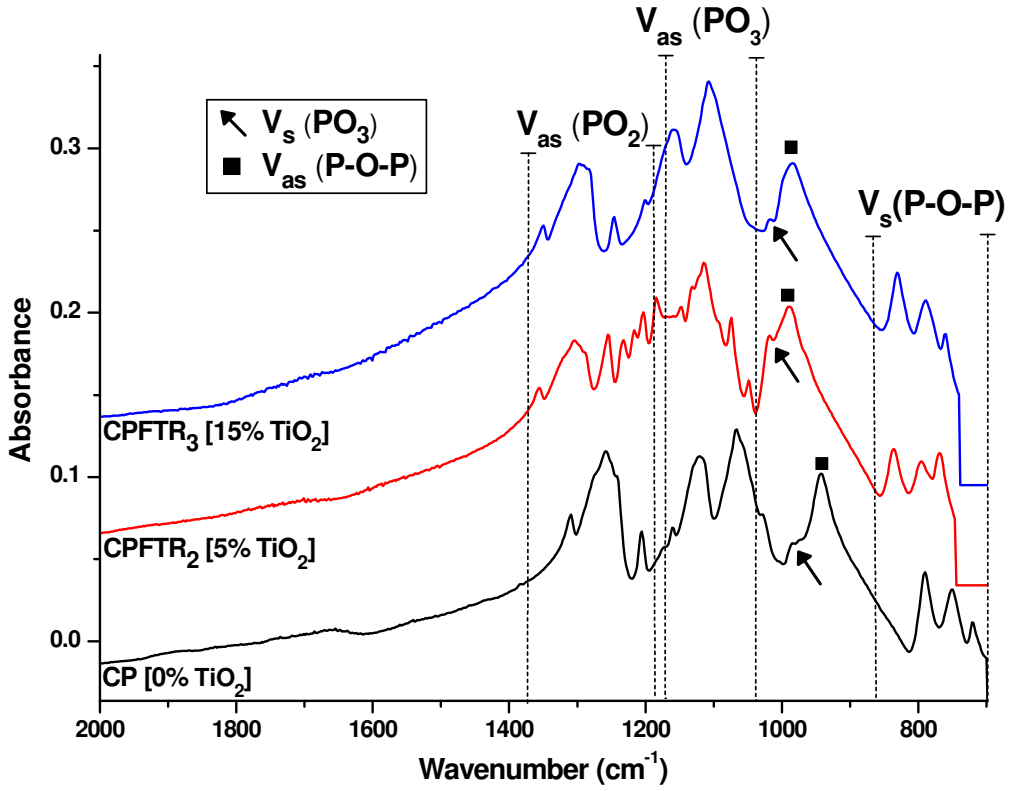

Figure 3.19: FTIR spectra of type A glass-ceramics.

The FTIR absorption spectra of type A glass-ceramics is shown in Figure 3.19 measured at room temperature. Table 3.11 gives further description of FTIR spectra of type A glass-ceramics.

Table 3.11: Description of FTIR spectra for type A glass-ceramics.

Wavenumber (cm^{-1})	**CP** [0 % TiO_2, 25 % CaF_2]	**CPFTR$_2$** [5 % TiO_2, 20 % CaF_2]	**CPFTR$_3$** [15 % TiO_2, 10 % CaF_2]	**Description**
	1205-1310	1200-1355	1248-1349	Asymmetric stretching vibrations of PO_2 [53]
	1067-1120	1048-1147	1109-1159	Asymmetric stretching vibrations of PO_3 [53]
	977	1019	1017	Symmetric stretching vibrations of PO_3 [52-54]
	942	988	986	Asymmetric stretching vibrations of P-O-P linkages [53]
	720-793	770-838	762-833	P–O–P symmetric stretch [51-52, 54-55]

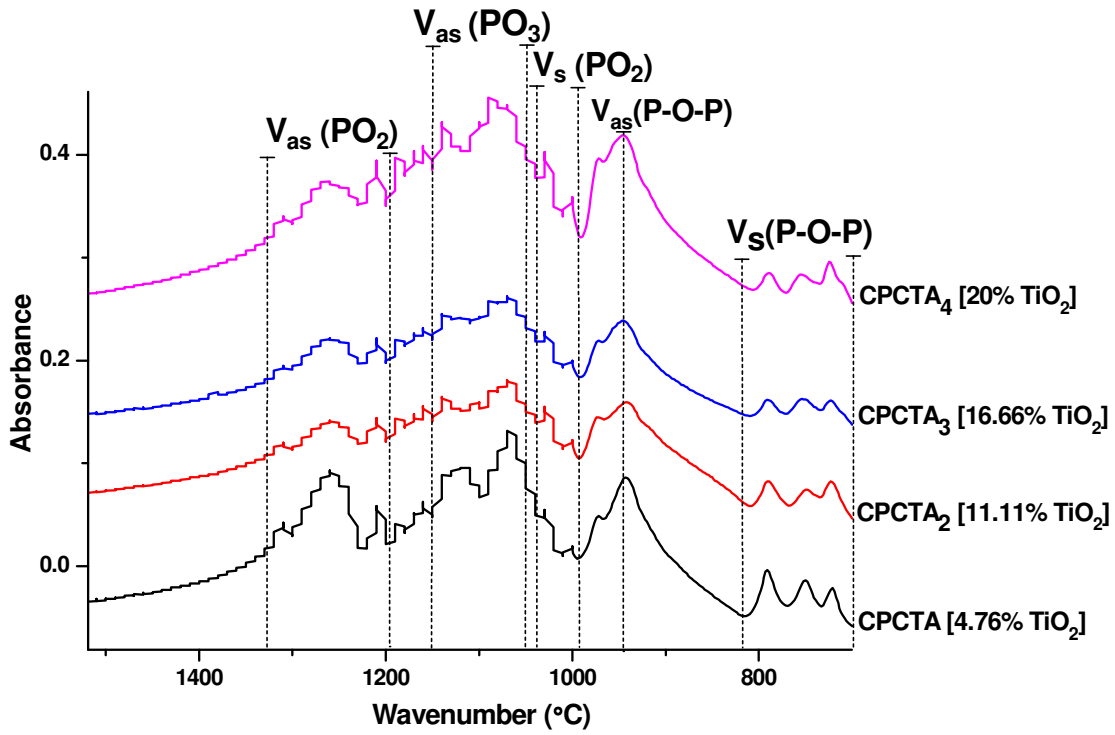

Figure 3.20: FTIR spectra of type B glass-ceramics

The FTIR absorption spectra of type B glass-ceramics are shown in Figure 3.20 measured at room temperature. Table 3.12 gives further description of FTIR spectra of type B glass-ceramics.

Table 3.12: Description of FTIR spectra for type B glass-ceramics.

	CPCTA [4.76 % TiO_2, 23.8% CaF_2]	CPCTA$_2$ [11.11 % TiO_2, 22.2% CaF_2]	CPCTA$_3$ [16.66 % TiO_2, 20.8% CaF_2]	CPCTA$_4$ [20 % TiO_2, 20 % CaF_2]	Description
Wavenumber (cm^{-1})	1208-1310	1211-1307	1214-1307	1211-1309	Asymmetric stretching vibrations of PO_2 [53]
	1065-1126	1067-1135	1068-1130	1070-1137	Asymmetric stretching vibrations of PO_3 [53]
	998-1038	999-1040	998-1040	1000-1038	PO_2^- symmetric groups [55]
	943	946	946	946	Asymmetric stretching vibrations of P-O-P linkages [53]
	722-793	722-790	722-793	725-790	P–O–P symmetric stretch [51-52, 54-55]

3.6 Thermogravimetric Analysis

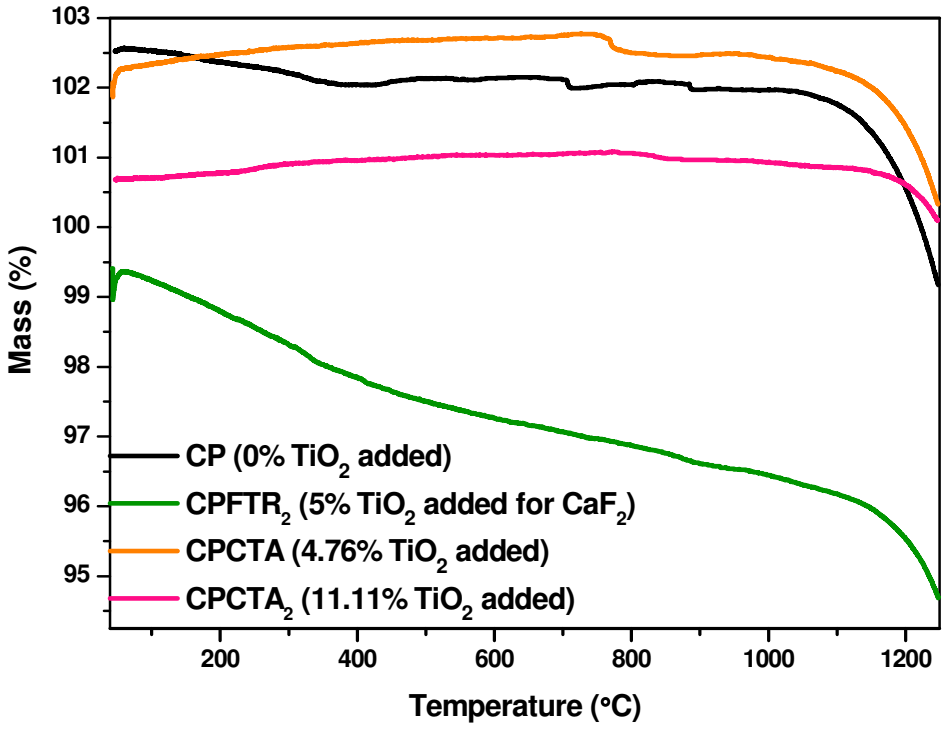

Figure 3.21: Thermogravimetric analysis of type A and B amorphous glasses only

Table 3.13: TGA results of type A and type B amorphous glasses

	CP (0 mol % TiO_2)	**$CPFTR_2$ (5 mol % TiO_2)**	**CPCTA (4.76 mol % TiO_2)**	**$CPCTA_2$ (11.11 mol % TiO_2)**
Type A Glass	√	√		
Type B Glass			√	√
Mass Used (mg)	11.91	11.76	11.92	11.78
Mass Loss (%)	3.39	4.73	1.58	0.61

3.7 Environmental Scanning Electron Microscopy Study

ESEM images produced from both type A and B glass-ceramics are shown in Figures 3.22 to 3.35 below.

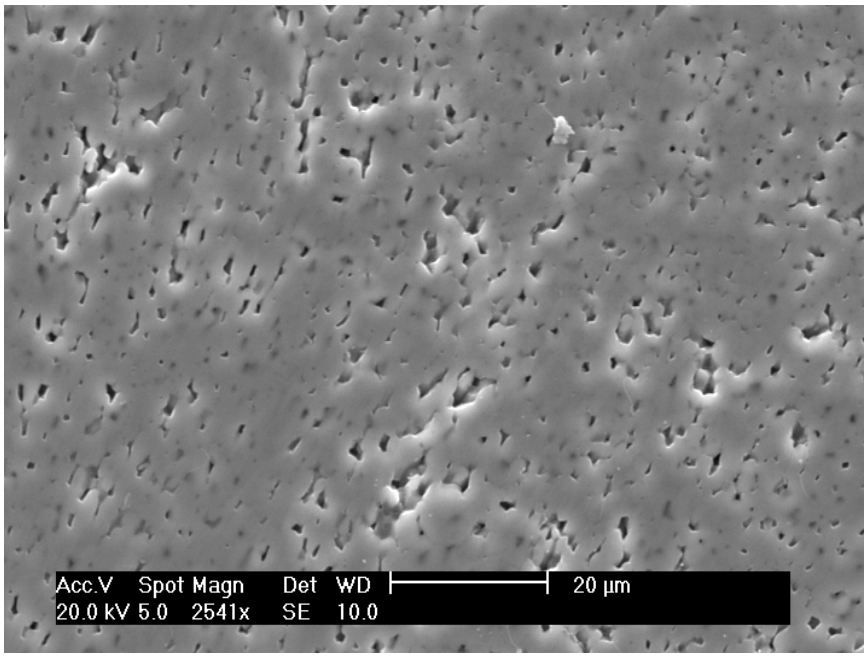

Figure 3.22: ESEM image of the surface of type A glass-ceramic, CP

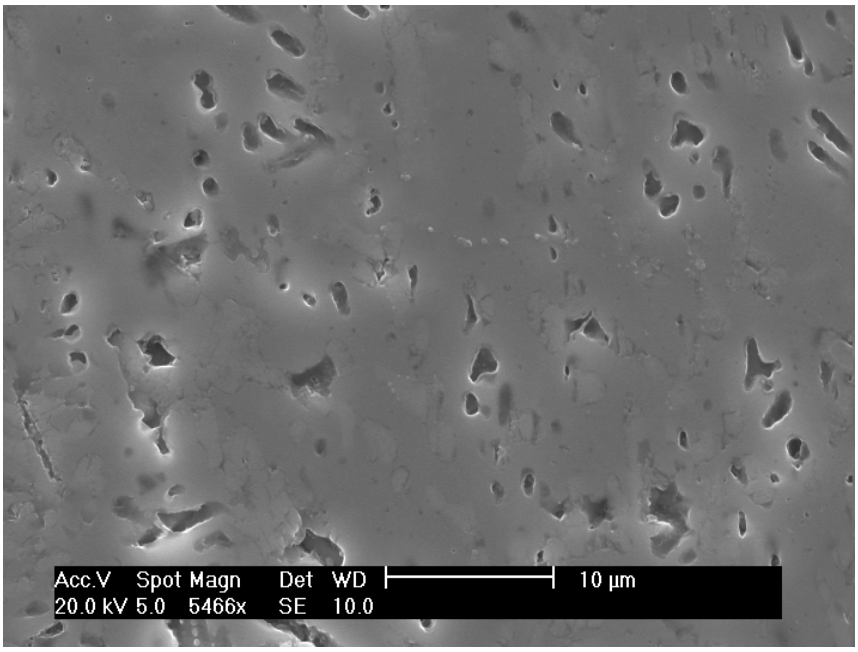

Figure 3.23: ESEM image of the surface of type A glass-ceramic, $CPFTR_2$

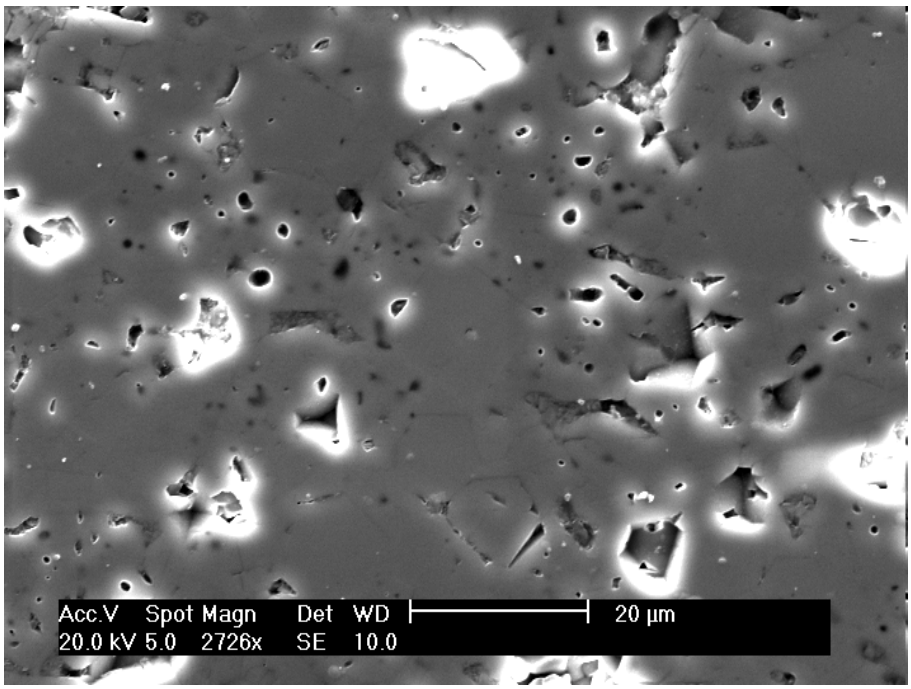

Figure 3.24: ESEM image of the surface of type A glass-ceramic, $CPFTR_3$

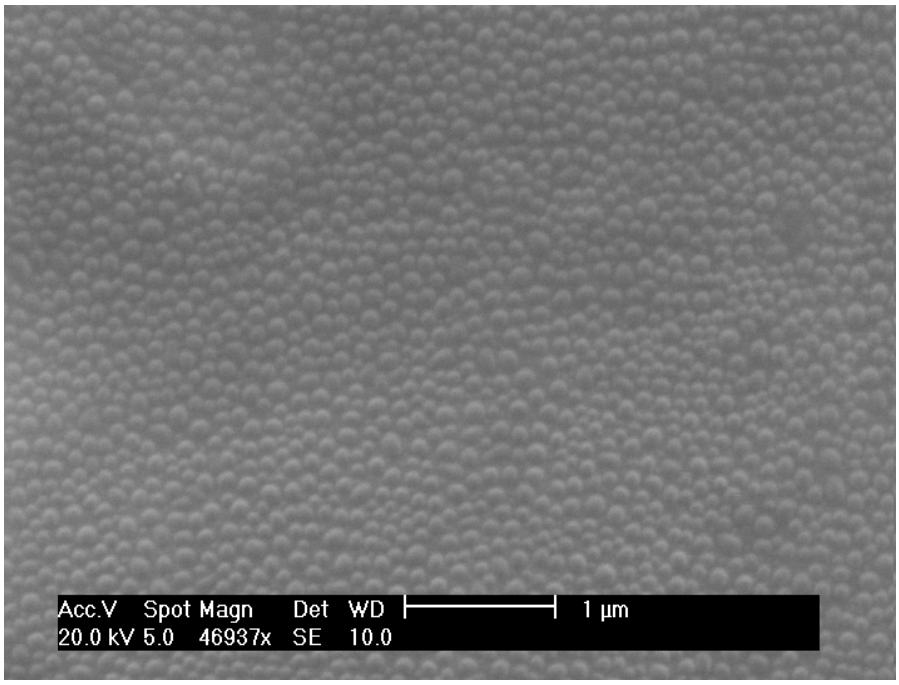

Figure 3.25: ESEM image of the surface of type A glass-ceramic $CPFTR_2$

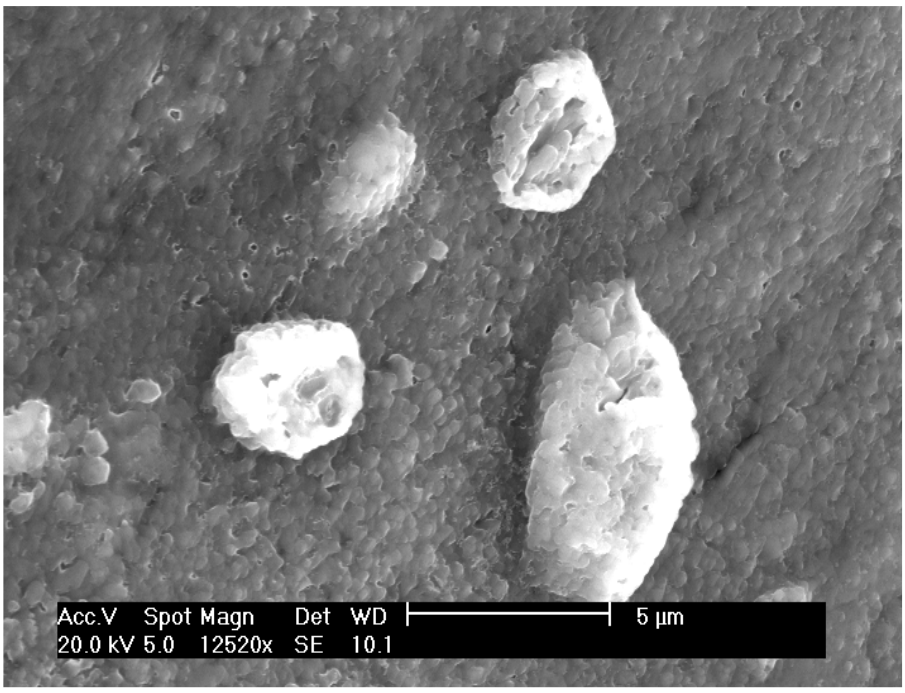

Figure 3.26: ESEM image inside a pore of type A glass-ceramic $CPFTR_3$

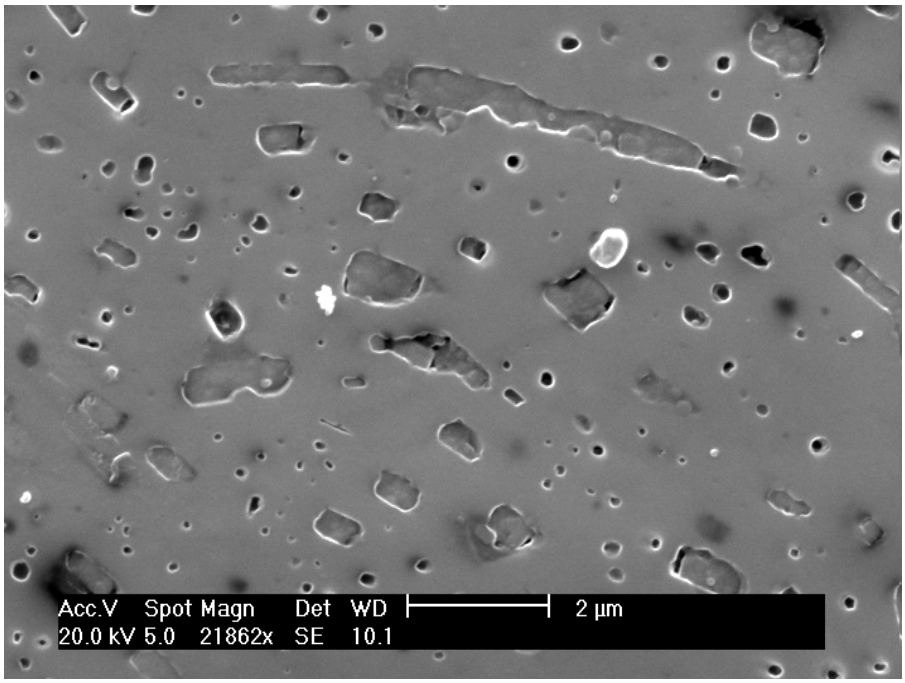

Figure 3.27: ESEM image of the surface of type B glass-ceramic CPCTA

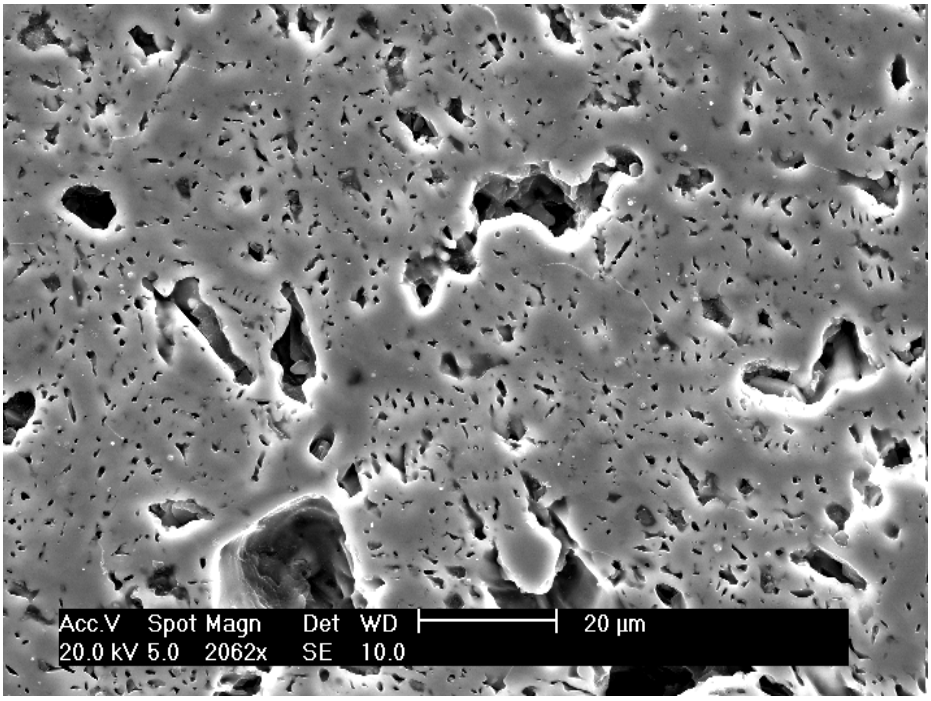

Figure 3.28: ESEM image of the surface of type B glass-ceramic $CPCTA_2$

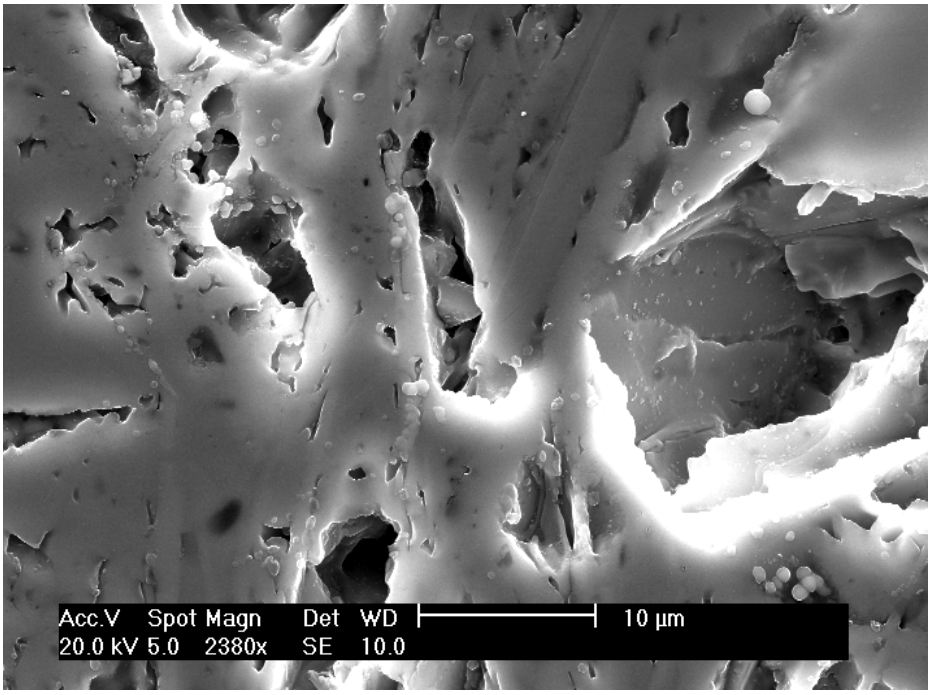

Figure 3.29: ESEM image of the surface of type B glass-ceramic $CPCTA_3$

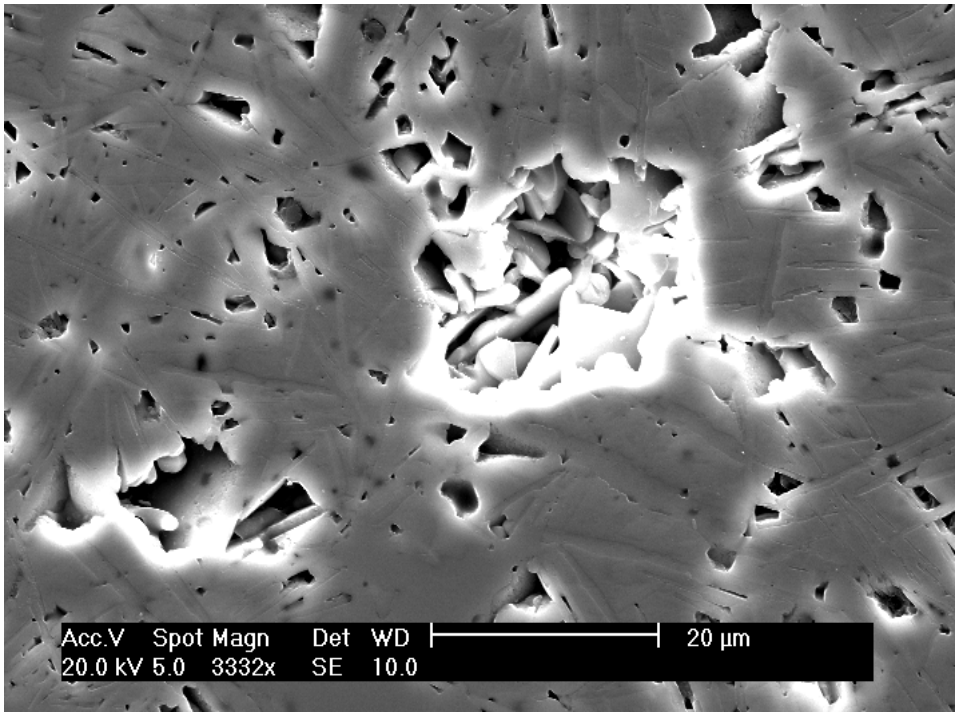

Figure 3.30: ESEM image of the surface of type B glass-ceramic $CPCTA_4$

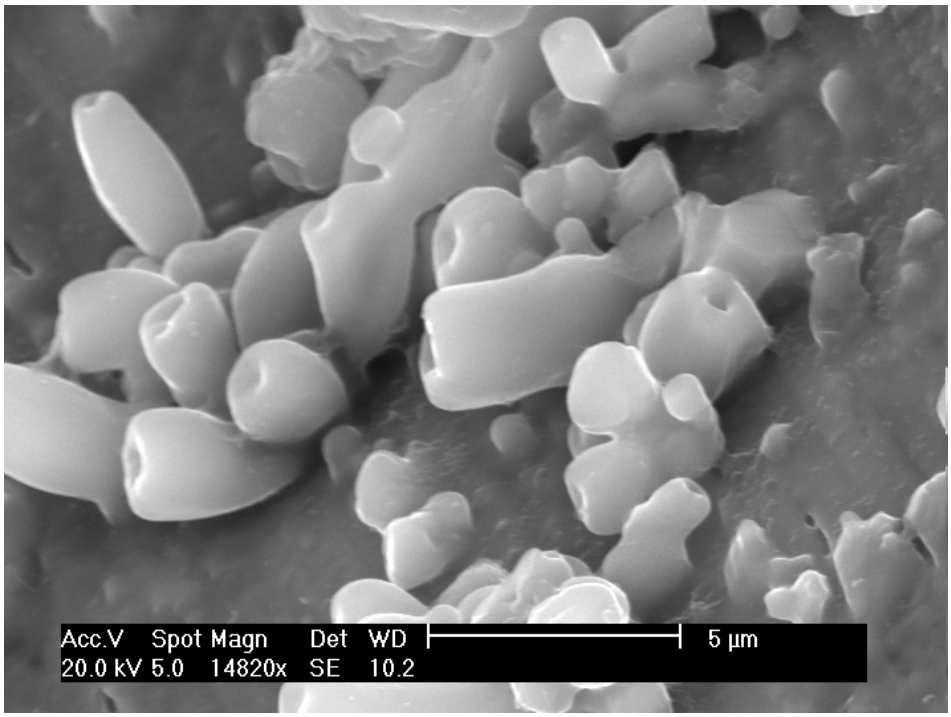

Figure 3.31: ESEM image inside a pore of type B glass-ceramic CPCTA

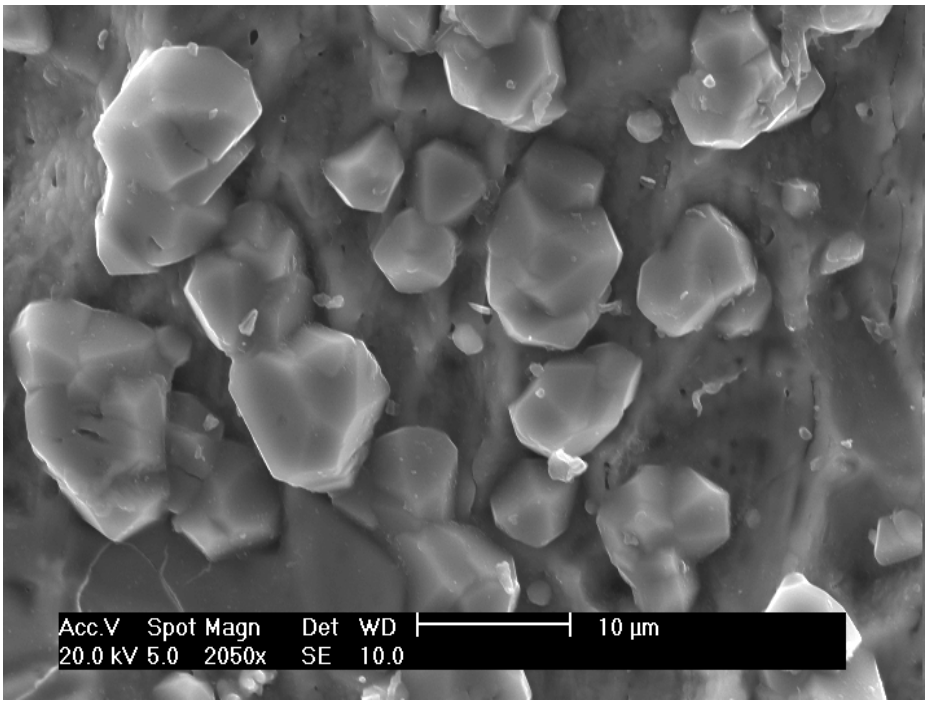

Figure 3.32: ESEM image inside a pore of type B glass-ceramic $CPCTA_2$

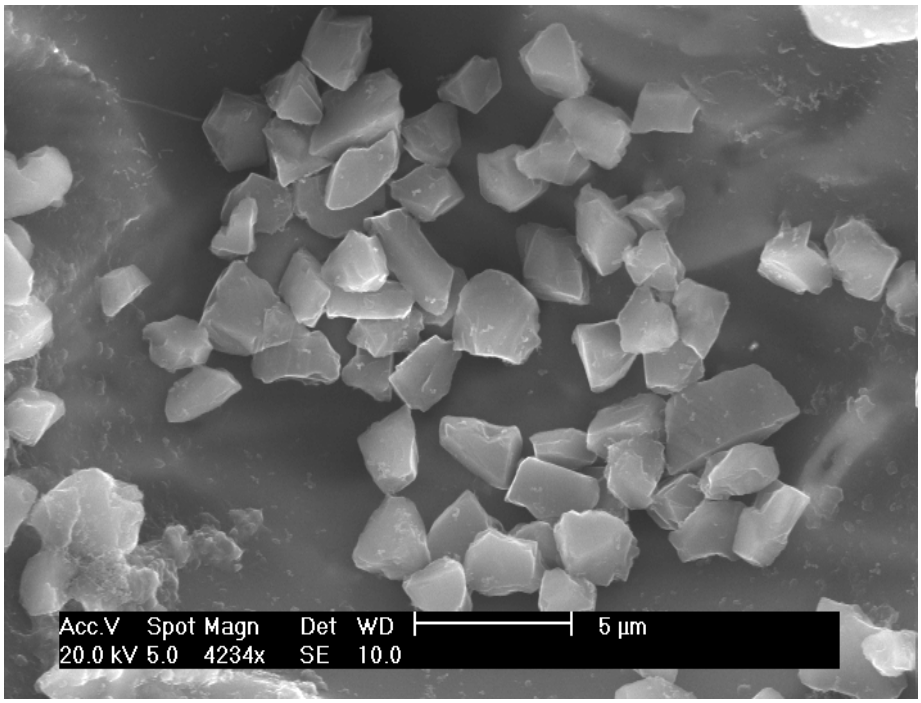

Figure 3.33: ESEM image inside a pore of type B glass-ceramic $CPCTA_3$

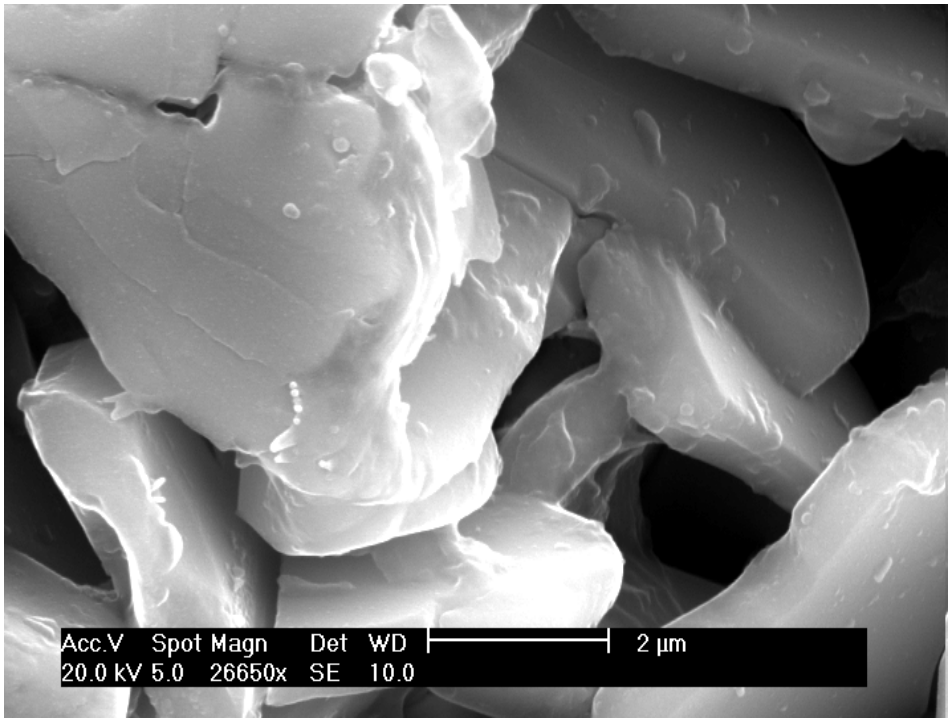

Figure 3.34: ESEM image inside a pore of type B glass-ceramic $CPCTA_4$

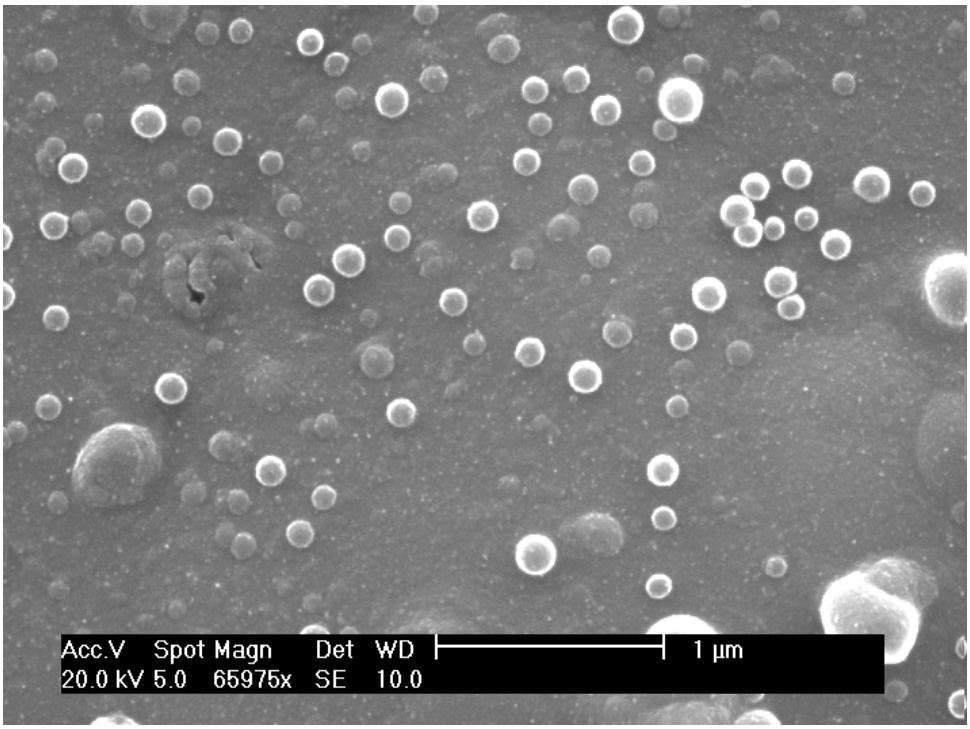

Figure 3.35: ESEM image on the surface of type B glass-ceramic $CPCTA_2$

3.8 Energy Dispersive X-ray Analysis of Glass and Glass-ceramics

The EDX analysis conducted on the glasses presented the actual composition of the glasses and the glass-ceramics after synthesis. Tables 3.14 to 3.17 show EDX results of the glass and glass-ceramics.

Table 3.14: EDX of type A glasses

Element	O	Ca	P	Ti	F	Total atomic %
Nominal composition of CP (at %)	66.67	11.11	22.22	-	-	100
Resulting composition of CP (at %)	*65.57*	*11.12*	*23.31*	-	-	100
Nominal composition of $CPFTR_2$ (at %)	60	9.47	21.05	1.05	8.42	100
Resulting composition of $CPFTR_2$ (at %)	*67.76*	*10.57*	*20.52*	*1.15*	-	100
Nominal composition of $CPFTR_3$ (at %)	64.2	7..37	21.05	3.16	4.21	100
Resulting composition of $CPFTR_3$ (at %)	*63.54*	*11.42*	*23.91*	*0.31*	*0.82*	100

Table 3.15: EDX of type B glasses

Element	O	Ca	P	Ti	F	Total atomic %
Nominal composition of CPCTA (at %)	63.09	10.73	21.46	0.43	4.29	100
Resulting composition of CPCTA (at %)	*67.09*	*10.92*	*21.56*	*0.43*	-	100
Nominal composition of $CPCTA_2$ (at %)	63.16	10.53	21.05	1.05	4.21	100
Resulting composition of $CPCTA_2$ (at %)	*62.06*	*12.04*	*23.48*	*1.31*	*1.11*	100
Nominal composition of $CPCTA_3$ (at %)	63.22	10.33	20.66	1.65	4.13	100
Resulting composition of $CPCTA_3$ (at %)	*62.17*	*11.38*	*23.39*	*1.13*	*1.93*	100
Nominal composition of $CPCTA_4$ (at %)	63.27	10.20	20.41	2.04	4.08	100
Resulting composition of $CPCTA_4$ (at %)	*64.82*	*10.92*	*21.20*	*1.65*	*1.40*	100

Table 3.16: EDX of type A glass-ceramics

Element	O	Ca	P	Ti	F	Total atomic %
Nominal composition of CP (at %)	66.67	11.11	22.22	-	-	100
Resulting composition of CP (at %)	*68.46*	*10.56*	*20.98*	-	-	*100*
Nominal composition of $CPFTR_2$ (at %)	60	9.47	21.05	1.05	8.42	100
Resulting composition of $CPFTR_2$ (at %)	*66.42*	*9.37*	*22.27*	*1.94*	-	*100*
Nominal composition of $CPFTR_3$ (at %)	64.2	7..37	21.05	3.16	4.21	100
Resulting composition of $CPFTR_3$ (at %)	*66.03*	*10.91*	*22.72*	*0.34*	-	*100*

Table 3.17: EDX of type B glass-ceramics

Element	O	Ca	P	Ti	F	Total atomic %
Nominal composition of CPCTA (at %)	63.09	10.73	21.46	0.43	4.29	100
Resulting composition of CPCTA (at %)	*68.05*	*10.52*	*21.07*	*0.37*	-	*100*
Nominal composition of $CPCTA_2$ (at %)	63.16	10.53	21.05	1.05	4.21	100
Resulting composition of $CPCTA_2$ (at %)	*65.28*	*12.70*	*21.19*	*0.83*	-	*100*
Nominal composition of $CPCTA_3$ (at %)	63.22	10.33	20.66	1.65	4.13	100
Resulting composition of $CPCTA_3$ (at %)	*66.43*	*11.09*	*20.94*	*1.54*	-	*100*
Nominal composition of $CPCTA_4$ (at %)	63.27	10.20	20.41	2.04	4.08	100
Resulting composition of $CPCTA_4$ (at %)	*64.29*	*12.74*	*21.57*	*1.40*	-	*100*

CHAPTER 4

4. Discussion

4.1 Manufacture of Glass

In the manufacturing of the type A glasses, only glass CP (0 % TiO_2) and $CPFTR_2$ (5 % TiO_2) came out as amorphous glasses. Glass $CPFTR_3$ (15 % TiO_2) was crystallised upon cooling. With the type B glasses, glass CPCTA (4.76 % TiO_2) $CPCTA_2$ (11.11 % TiO_2) both were amorphous glasses whereas glasses $CPCTA_3$ (16.66 % TiO_2) and $CPCTA_4$ (20 % TiO_2) were both crystallised upon cooling. Both type A and B glasses were melted upto 1200°C during the manufacturing of the glasses. Although it was apparent from the DSC results, that the main melting temperature for type A glasses was in the region 967-976°C and for type B glasses, 963-978°C and hence was lower than the 1200°C, it was necessary to use this higher melting temperature in order to achieve the required viscosity to permit fusion of all the oxides so the glass could be made.

4.2 Differential Scanning Calorimetry Analysis

The glass transition temperature (Tg), crystallization temperatures (Tp) and melting temperatures (Tm) values of type A glasses can be seen in Table 3.3. There was an increase in the glass transition temperatures in type A glasses, when TiO_2 addition for CaF_2 upto 5 mol % took place, from 550^{o}C for CP (0 mol % TiO_2) to 572^{o}C for $CPFTR_2$ (5 mol % TiO_2). However once 15 mol % TiO_2 was added for CaF_2 then a decrease was observed in the Tg to 538^{o}C for $CPFTR_3$. (Presented in figure 3.3). According to previous research carried out on calcium phosphate glasses which substituted sodium with increasing TiO_2 content, the glass transition temperature was expected to increase with increasing content of upto 15 mol % TiO_2. [14, 47, 52] It has been reported [14, 47, 52] that in calcium phosphate glasses containing TiO_2, an increase

in Tg was observed as TiO_5 (tetragonal pyramidal) or TiO_6 (distorted octahedral) titanate polyhedra and P-O-Ti bonds were formed [52]. Moreover, an increase in Tg was observed if the ion was of a smaller ionic radius compared with the ion being substituted. Hence in this case, the increase in Tg from glass CP to $CPFTR_2$ may possibly be due to the ionic radius of Ti (0.068 nm) being smaller than the ionic radius of calcium (0.114 nm) and having a larger electrical charge, therefore when it penetrates the glass network interstices, the titanate polyhedra causes the cross link density to be increased which in turn causes an increase in the Tg. [14, 47, 52] The significant decrease in Tg in glass $CPFTR_3$ (15 mol % Ti) was due to the fact that Ca was being substituted by Ti and because there is a reduction in the Ca/P ratio here, it causes the decrease in Tg.

Similar changing tendency was found with the trend in crystallization temperatures for these glasses. In comparison to the rest of the type A glasses, only glass $CPFTR_2$ (5 mol % TiO_2) exhibited two crystallization peaks, the second being much more intense than the first peak and hence the intense peak can be considered as the main crystallization temperature. (This can be seen in figure 3.1). The fact that two crystallization peaks were observed in $CPFTR_2$ was in agreement with previous studies. [47, 52] This suggests that Ti acts as a nucleating agent, when a certain amount of Ti is added and it induces phase separation upon cooling of the molten glass. [52] The main crystallization peak temperature increased significantly when TiO_2 was added for CaF_2 of upto 5 mol % from 672^{o}C for CP (0 mol % TiO_2) to 770^{o}C for $CPFTR_2$ (5 mol % TiO_2) and again when 15 mol % TiO_2 added for the CaF_2; there was a significant decrease to 682^{o}C for $CPFTR_3$. (Presented in figure 3.4) We expected to see two crystal phases (including titanium pyrophosphate) in $CPFTR_2$ and $CPFTR_3$ whereby both phases would have crystallised at a similar temperature to

titanium pyrophosphate; however the results from the DSC show that this was not the case.

Similar changing tendency is again found on the main melting peak temperatures. The main melting peak temperature increased slightly from 972°C for CP (0 mol % TiO_2) to 976°C for $CPFTR_2$ (5 mol % TiO_2) and then decreased to 967°C for $CPFTR_3$ (15 mol % TiO_2). (Presented in figure 3.5). Only glass $CPFTR_2$ exhibited two melting peaks, the first was a smaller broader peak than the second peak, which was more intense and hence was considered to be the main one. This can be seen from figure 3.1. Therefore the change in melting temperature was not significant overall and could be attributed to the two crystal phases present in the glass.

The glass transition temperature (Tg), crystallization temperature (Tp) and melting temperature (Tm) values of type B glasses can be seen in Table 3.4. Both the glass transition temperatures for type B glasses followed a similar changing tendency as the type A glasses. Tg_1 and Tg_2 increased when TiO_2 was added upto 11.11 mol % from 546°C (CPCTA) to 570°C ($CPCTA_2$) for the first glass transition temperature and from 779°C (CPCTA) to 810°C ($CPCTA_2$) for the second glass transition temperature, however when 16.66 mol % TiO_2 was added, both Tg_1 and Tg_2 decreased to 551°C and 787°C ($CPCTA_3$) respectively. Furthermore, addition of 20 mol % TiO_2 caused an increase in Tg_1 and Tg_2 to 569°C and 811°C ($CPCTA_4$) respectively. (This can be seen in figures 3.9-3.10). It was expected that an increase in TiO_2 content would increase the Tg due to the fact that addition of TiO_2 results in an increase in the glass viscosity and strengthens the glass network, possibly by the formation of TiO_5 or TiO_6 structural units and the formation of P–O–Ti bonds which then forms ionic cross-linking between the non-bridging oxygen of two different chains which consequently strengthens the glass structure as mentioned earlier. However in the case of glass

$CPCTA_3$ (16.66 mol % TiO_2), a decrease in both the Tg's was observed, and as this decrease was less than 25°C it can be attributed to the two amorphous phases which were present in the glass.

A similar changing tendency occurs for the main crystallization peak temperatures for these glasses. Glasses CPCTA (4.76 % TiO_2) and $CPCTA_2$ (11.11 % TiO_2) were the only glasses which exhibited two crystallization peaks whereas the other glasses exhibited a single crystallization peak. Glass CPCTA exhibits a less intense peak after the main intense crystallization peak whereas glass $CPCTA_2$ exhibits a less intense peak before the main intense crystallisation peak. In both cases, the most intense peak is regarded as the main crystallization temperature peak. (This can be seen from figure 3.6). This again can be attributed to the fact that TiO_2 can act as a nucleating agent, when a certain amount of TiO_2 is added into the glasses and that it induces phase separation upon cooling of the molten glass. [52] There was a significant increase in the crystallization temperature from 698°C in CPCTA (4.76 mol % TiO_2) to 777°C in $CPCTA_2$ (11.11 mol % TiO_2) and then there was a decrease to 720°C in $CPCTA_3$ (16.66 % TiO_2) and again there was an increase to 751°C in $CPCTA_4$ (20 % TiO_2). (This can be seen from figure 3.11). A study by Lee et al (1999) has confirmed that addition of TiO_2 affects the nucleation behaviour of calcium phosphate glasses and has reported that increasing the TiO_2 content will result in an increase in the crystallization temperature. [45] However glass $CPCTA_3$ did not follow this increasing trend and rather it decreased. Furthermore, glass $CPCTA_4$ increased slightly but its value was still not higher than the value for the highest Tp value observed in glass $CPCTA_2$. This was because the glass phase formed crystallised at a much lower temperature and that the crystalline phase, titanium pyrophosphate therefore had a significant effect on the glass and this was demonstrated by the change in Tp. As can be seen from Figure 3.6, when more TiO_2 was added from glasses CPCTA to

$CPCTA_4$ the main crystallization peak became less intense and broader, suggesting that there were different crystal sizes present, or multiple crystal phases that overlap were present. Furthermore, it was observed that the degree of crystallinity decreased and this was evident from XRD pattern of $CPCTA_4$, as its XRD peaks were shown to be less intense.

Glasses CPCTA, $CPCTA_2$ and $CPCTA_3$ all exhibited two melting peaks whereas $CPCTA_4$ only exhibited one melting peak. (This can be seen from figure 3.6). The main melting temperature increased, when TiO_2 added content increased, from 963^oC for CPCTA (4.76 mol % TiO_2) to 978^oC for $CPCTA_3$ (16.66 mol % TiO_2), however there was a decrease to 974^oC for $CPCTA_4$, when 20 mol % TiO_2 was added. (This can be seen from figure 3.12). Overall there wasn't a considerable change in the main melting temperature values of these glasses and therefore it can be attributed to the two crystal phases present in the glasses. The Tm of glass $CPCTA_4$ was also broader and less intense in comparison to the rest of the glasses which further confirmed the possibility of different crystal sizes present or multiple phases that overlap being present in the glass.

4.3 Density and Oxygen Density Analysis

The trend observed in the glass transition temperatures for type A and B glasses is similar to the trend followed in the density measurements for each of these glasses. For the type A glasses, the measured density value improved with introduction of TiO_2 from 2.6879 g/cm^3 for glass CP (0 mol % TiO_2) to 2.7471 g/cm^3 for glass $CPFTR_2$ (5 mol % TiO_2). However, a slight decrease was observed to 2.7259 g/cm^3 when 15 mol % TiO_2 was used in glass $CPFTR_3$ as shown in Figure 3.13. It can also be seen from this figure that although there was a slight decrease in density for glass $CPFTR_3$, this value was still higher than the density value for glass CP which did not

contain TiO_2. Therefore TiO_2 containing calcium phosphate glasses were denser than calcium phosphate glasses without TiO_2. The initial increase and then decrease in density was parallel with an increase in Tg initially and then when 15 mol % TiO_2 was added for CaF_2, there was a decrease in both Tg and density values. The initial increase in density is due to the fact that titanium has a slightly larger atomic weight (AW = 48) than the atomic weight of calcium (AW = 40). Another explanation could be that there is a possibility of TiO_5 (tetragonal pyramidal) or TiO_6 (distorted octahedral) being present as reported by Neel at al (2009) [52] and as the ionic radius of Ti (0.068nm) is smaller than the ionic radius of calcium (0.114 nm) and has a larger electrical charge, when penetrating the glass network interstices, the titanate polyhedra increase the atomic packing causing an increase in the density. [14, 47, 52] However, in the present study there was no evidence from the FTIR about the presence of titanate polyhedra. The decrease in density with the addition of 15 mol % TiO_2 for CaF_2 was not expected and cannot be explained. It was anticipated that TiO_2 addition for CaF_2 would lead only to an increase in density as mentioned above.

The calculated oxygen density was shown to decrease slightly with increasing TiO_2 content, from 0.2172 g/cm^3 for glass CP (0 mol % TiO_2) to 0.2081g/cm^3 for glass $CPFTR_3$ (15 mol % TiO_2). (This can be seen in figure 3.13). This decrease was consistent and demonstrated that TiO_2 disrupts the glass network due to the fact that the Ca/P decreases when the TiO_2 content increases and this was more of a significant effect than when TiO_2 was added to type B glasses whereby the Ca/P was kept constant at 0.5.

For the type B glasses, the measured density values improved with increasing TiO_2 content from 2.7072 g/cm^3 in glass CPCTA (4.76 mol % Ti) to 2.7584 g/cm^3 in glass $CPCTA_2$ (11.11 mol % Ti). A slight decrease in the density value to 2.7552 g/cm^3 occurred in glass $CPCTA_3$ when 16.66 mol % TiO_2 was added to the glass, which can

be seen in Figure 3.14. Then an increase was observed to 2.8061 g/cm^3 for glass $CPCTA_4$ (20 mol % TiO_2), this density value for $CPCTA_4$ was the highest density value when compared with the rest of the type B glasses. Therefore there was generally an increase in density with an increase in TiO_2 content, except in the case of glass $CPCTA_3$ the density only decreased very slightly and hence it was not classified as significant. This increase is due to the fact that titanium has a slightly larger atomic weight (AW = 48) than the atomic weight of calcium (AW = 40) as well as the possible formation of TiO_5 or TiO_6 titanate polyhedra as explained earlier. Furthermore, the ionic radius of Ti (0.068nm) is smaller than the ionic radius of calcium (0.114 nm) and has a larger electrical charge, therefore when penetrating the glass network interstices, the titanate polyhedra increases the atomic packing and hence causes an increase in the density. [14, 47, 52]

The oxygen density value increased from 0.0843 g/cm^3 for glass CPCTA (4.76 mol % TiO_2) to 0.0847 g/cm^3 for glass $CPCTA_2$ (11.11 mol % TiO_2) and then it slightly decreased to 0.0834 g/cm^3 for glass $CPCTA_3$ (16.66 mol % TiO_2) and then increased again to 0.0842 g/cm^3 for glass $CPCTA_4$ (20 mol % TiO_2). (This can be seen in figure 3.14). As there was only a minor change in oxygen density values of these TiO_2 added glasses, it suggests that TiO_2 addition does not have a significant effect on the glass-network.

4.4 X-Ray Diffraction Analysis

The XRD patterns of type A glass-ceramics can be seen in Figure 3.15 and the summary of the crystal phases are presented in Table 3.7. From this, it is observed that glass-ceramic CP, which did not contain TiO_2 was crystallised to calcium metaphosphate, (CaP_2O_6) and this was the only phase observed for this sample. There was also a change of the XRD pattern with substitution of TiO_2 for CaF_2, demonstrating the appearance of new phases in the crystallised glass samples.

Through comparison between our current XRD patterns and reference XRD patterns from the database it was observed that the introduction of TiO_2 caused new phases to emerge and that glasses $CPFT_2$ (5 mol % TiO_2) and $CPFT_3$ (15 mol % TiO_2) crystallised to calcium metaphosphate (CaP_2O_6), calcium pyrophosphate ($Ca_2P_2O_7$) and titanium pyrophosphate (TiP_2O_7). Glass-ceramic $CPFT_2$ had a small amount of TiP_2O_7 present compared with glass-ceramic $CPFT_3$. It was observed that as the TiO_2 content increased from glass-ceramic $CPFT_2$ (5 mol % TiO_2) to $CPFT_3$ (15 mol % TiO_2), the intensity of the CaP_2O_6 and TiP_2O_7 phase increased whilst the amount of $Ca_2P_2O_7$ formed decreased. It is reported that both $Ca_2P_2O_7$ and CaP_2O_6 phases are bioactive and non toxic. [57]

Our XRD patterns are not in full agreement with previous research conducted on a similar composition, as it was suggested by Kasuga et al. [41-42] that peaks assigned to Nasicon type crystal emerged, such as: $CaTi_4(PO_4)_6$, $Ti(PO_3)_3$ and $(TiO)_2P_2O_7$. Furthermore TiO_2, fluoroapatite and $Ca_2P_2O_7$ were also observed. From the present results, the only crystalline phase in agreement with previous research on the same composition was the calcium pyrophosphate, $Ca_2P_2O_7$ phase. [41-42]

However research conducted on calcium phosphate glass-ceramics containing sodium with the addition of TiO_2 are in good agreement with present results as they have also found CaP_2O_6 to be the main crystal phase as well as observing TiP_2O_7 as a secondary phase. [52] Furthermore, calcium pyrophosphate, $Ca_2P_2O_7$ crystalline phases were also found in this type of glasses, which is again in agreement with our results. [33, 35, 37] Moreover, calcium phosphate glass-ceramics containing magnesium with TiO_2 has also shown to have crystalline phases in agreement with our results as they have found phases such as $Ca_2P_2O_7$ and TiP_2O_7. [27, 31, 34, 45]

From the XRD patterns of type B glass-ceramics seen in Figure 3.16 and the summary of the crystal phases present in Table 3.8, it was apparent that all glasses CPCTA, $CPCTA_2$, $CPCTA_3$ and $CPCTA_4$ were crystallised to calcium metaphosphate, CaP_2O_6, which was the main phase as well as calcium pyrophosphate, $Ca_2P_2O_7$ and titanium pyrophosphate, TiP_2O_7 being secondary phases. The glass-ceramic CPCTA (4.76 mol % TiO_2) had only a small amount of TiP_2O_7 formed in comparison to the rest of the materials. Similarly to the XRD patterns of type A glass-ceramics, the intensity of the crystalline phase, TiP_2O_7 increased with increasing TiO_2 content, which was expected. However the intensity of the crystalline phases, CaP_2O_6 and $Ca_2P_2O_7$ both decreased with increasing TiO_2 content in these type B glass-ceramics. Although the decrease in $Ca_2P_2O_7$ for type B glass-ceramics was in good agreement with the XRD patterns of type A glass-ceramics, the decrease in CaP_2O_6 has shown to be in disagreement as there was an increase in CaP_2O_6 observed in type A glass-ceramics when increasing the amount of TiO_2 added rather than a decrease which was observed in type B glass-ceramics.

Again our XRD results are not in good agreement with previous research carried out on the same composition and only one crystalline phase was in agreement to previous research which was $Ca_2P_2O_7$. [41-42] However, XRD patterns from calcium phosphate glass-ceramics containing sodium with TiO_2 addition have shown to be in good agreement with our results [33, 35, 37, 52] as well as with calcium phosphate glasses containing magnesium and TiO_2. [27, 31, 34, 45]

In both the type A and B glass-ceramics, a fluorine containing crystalline phase was not observed and this was also confirmed by the EDX results which showed that no fluorine was retained in both types of glass-ceramics, which was disappointing.

4.5 Fourier Transform Infrared Spectroscopy Analysis

The FTIR absorption spectra for type A glasses is shown in figure 3.17 and displays peaks corresponding to the metaphosphate group, (asymmetric stretch of PO_2; 1255-1285cm^{-1}) orthophosphate group (symmetric stretch of PO_4^{3-} 960-1060cm^{-1}), and pyrophosphate group, (asymmetric stretch of PO_3; 1085-1090cm^{-1}). Moreover, all type A glasses shows peaks corresponding to bending vibrations of P-O-P linkages (474-496cm^{-1} and asymmetric vibrations of P-O-P linkages 903-908cm^{-1}) and a very small peak corresponding to the symmetric stretching vibrations of P-O-P bridges (745-750cm^{-1}). It is observed from the spectra that only glass $CPFTR_3$, whereby 15 mol % TiO_2 is added for CaF_2, exhibits a very small peak corresponding to the Ti-O-Ti symmetric stretch (760-790cm^{-1}), a very small peak corresponding to PO_4^{3-} bending (560cm^{-1}) and a peak corresponding to $P_2O_7^{4-}$ (535cm^{-1}). [35, 50-56] Our results are in some agreement with previous research, as peaks corresponding to meta-phosphate and pyrophosphate groups without the orthophosphate group were observed in calcium phosphate glasses containing TiO_2. [50, 52, 57] It can be seen that the intensity of peaks that correspond to the metaphosphate group ($PO_{2[as]}$), orthophosphate group ($PO_4^{3-}{}_{[s]}$) and pyrophosphate group ($PO_{3[as]}$ and P-O-$P_{[s]}$ stretch) increase as the addition of TiO_2 content increases, from glass CP (0 mol % TiO_2) to glass $CPFTR_3$ (15 mol % TiO_2). This is not in complete agreement with previous research because with increasing TiO_2 content; one would expect an increase in intensity of peaks corresponding to the pyrophosphate group and a decrease in peaks corresponding to the metaphosphate groups due to the fact that incorporation of Ti ions into the phosphate network causes a structural change as the phosphate network changes from chain extending metaphosphate tetrahedra to chain-terminating pyrophosphate groups, which is expected when the O:P ratio increases in glasses. [14, 47] However the disagreement lies in the fact that our results showed an increase in

intensity of peaks relating to metaphosphate groups, rather than a decrease. Alternatively the intensity of the peak corresponding to the asymmetric stretch of the P-O-P vibration (903-908 cm^{-1}) broadens and shifts to a higher wavenumber as the addition of TiO_2 content increases from glass CP to glass $CPFTR_3$ which was expected as this was evidence that the phosphate chains were strengthened, by introduction of titanium ions. [52]

The FTIR absorption spectra of type B glasses is shown in figure 3.18 and it displays peaks corresponding to the metaphosphate group (asymmetric stretch of PO_2; 1275-1282cm^{-1}), orthophosphate group, (symmetric stretch of PO_4^{3-}; 961-1021 cm^{-1}) and pyrophosphate group, (asymmetric stretch of PO_3; 1084-1091cm^{-1}). Furthermore, all type B glasses show peaks corresponding to the asymmetric stretching of P-O-P linkages (901-904cm^{-1}) as well as a small peak corresponding to the symmetric stretches of P-O-P bridges (725-778cm^{1}). It is observed that the intensity of the peaks which correspond to the metaphosphate group ($PO_{2[as]}$) and pyrophosphate group ($PO_{3[as]}$) decrease when TiO_2 content increases upto 11.11 mol % from glasses CPCTA (4.76 mol % TiO_2) to $CPCTA_2$ (11.11 mol % TiO_2) and then for glass $CPCTA_3$ (16.66 mol % TiO_2), the intensity of these peaks increase and further on for glass $CPCTA_4$ (20 mol % TiO_2) they decrease again. Therefore generally, the peaks relating to metaphosphate and pyrophosphate groups decreased with the exception of glass $CPCTA_3$ (16.66 mol % TiO_2) which showed an increase. The decrease observed in the metaphosphate group peak is in agreement with previous research. However the decrease in the peak corresponding to pyrophosphate group is not in agreement as it was expected for it to increase as the TiO_2 content increased, but it only increased in the case of $CPCTA_3$. The expected increase in pyrophosphate group peaks and decrease in metaphosphate group peaks is because the Ti ions cause a structural change in the phosphate network as explained earlier; hence there is a

change from metaphosphate to pyrophosphate groups. [14, 47, 52] Furthermore, the intensity of the peak attributed to PO_4^{3-}(s) increase and shift to lower wavenumbers when then TiO_2 content increases.

Comparing both FITR absorption spectra of type A and type B glasses with one another, it is observed that both spectra for each of the glasses displayed a lack of sharp peaks overall, suggesting that there was disorder in the phosphate network. Both the spectra exhibited peaks corresponding to the metaphosphate, pyrophosphate and orthophosphate groups. The metaphosphate region in both spectra was assigned to the asymmetric stretch of PO_2 whereby the two non-bridging oxygen atoms are bonded to a phosphorus atom in a Q^2 phosphate tetrahedron. The pyrophosphate region was assigned to the asymmetric stretch of PO_3. The orthophosphate region was assigned to the symmetric stretch of the PO_4^{3-} group whereby the non bridging oxygen atoms are bonded to a phosphorus atom in Q^0 phosphate tetrahedra. Moreover, both spectra exhibited peaks corresponding to the asymmetric vibrations of P-O-P linkages, as well as showing small peaks assigned to the symmetric stretching of P-O-P bridges.

The FTIR absorption spectra of type A and B glass-ceramics are shown in Figures 3.19-3.20. Both spectra exhibit peaks corresponding to metaphopshate ($PO_{2[as]}$), pyrophosphate ($PO_{3[as]}$) as well as P-O-$P_{[s]}$) and P-O-$P_{[as]}$. Type A glass-ceramic spectra exhibits another peak which was not present in the type B glass-ceramic spectra which coincides with $PO_{3[s]}$ stretch.

In both spectra of the glass-ceramics there were no bands relating to Ti-O-Ti linkages, which suggested that titanium ions were consumed during the formation of a crystalline phase such as TiP_2O_7, confirmed by XRD patterns. [42] In comparison to the spectra's of the glasses, these spectra showed that peaks relating to metaphosphate

($PO_{2[as]}$) and pyrophosphate groups ($PO_{3[as]}$) as well as P-O-$P_{[s]}$ were decomposed into several narrow peaks in the spectra of the glass-ceramics. It has been reported that the spectra of heat treated calcium phosphate glasses were seen to consist of several narrow peaks relating to metaphosphate and pyrophosphate groups, compared with the original glasses, which is in agreement with our results. [53] Moreover, in the type A glass-ceramics FTIR absorption spectra, there was a shift of all peaks to higher wavenumbers with the introduction of TiO_2, suggesting that Ti ions cause a structural disorder in the network, as explained earlier.

4.6 Thermogravimetric Analysis

Table 3.13 summarises the results from TGA on the amorphous glass samples only. For the type A glasses, it was observed that glass CP (0 mol % TiO_2) had a mass loss of 3.39% and for glass $CPFTR_2$ (5 mol % TiO_2 added for CaF_2) had a mass loss of 4.73%, which was quite high in comparison with the rest of the glass samples. Fluorine was not retained in this glass, this was confirmed by XRD analysis whereby no fluorine containing phases were present. EDX analysis which has shown that fluorine was not retained in both these glasses is also in agreement with the above.

For the type B glasses, for glass CPCTA (4.76 mol % TiO_2 added) the mass loss observed was 1.58% which was not as high as the previous mass loss observed and therefore we expected a small amount of fluorine to be retained in the glass, however this was not the case and it was not retained in the glass. This observation cannot be explained. For glass $CPCTA_2$ (11.11 mol % TiO_2 added), only small amount of mass loss of 0.61% was seen and hence fluorine was expected to remain in this glass which was the case and this was confirmed by EDX analysis.

From the TGA results in type A glasses when the TiO_2 content is 5 mol % as in the case of glass $CPFTR_2$ there was a significant mass reduction with increasing temperature, however with the rest of the glasses no significant mass reduction with increasing temperature was observed. Mass reduction was not expected to be observed. Considering the very small increase in density during crystallisation, it was expected that no significant mass change should be observed in the TGA analysis. On the other hand the 5 % TiO_2 containing type A glass seems to undergo significant fluorine loss during this process taking into consideration also the EDX results where no fluorine was observed for the glass-ceramic. It can be concluded that by analysing TGA and EDX results, it seems that fluorine is retained in the amorphous type A and type B glasses except in the case of $CPFTR_2$ (5 % Ti) and CPCTA (4.76 % Ti). It was expected for fluorine to remain in both these glasses too. Therefore a small amount of fluorine is retained in the amorphous phase but not in the crystalline phase and this suggests that fluorine does escape possibly as CaF_2.

4.7 Environmental Scanning Electron Microscopy Analysis

From the ESEM images, it can be seen that in type A glass-ceramics (Figures 3.22 to 3.24) and in type B glass-ceramics (Figures 3.27 to 3.30), many independent pits which were several tens of nanometers in size were observed. The independent pits observed were larger in type B glass-ceramics. This observation is in agreement with Kasuga et al's previous research. [41-42] Kasuga et al. studied a calcium phosphate composition that after crystallisation the composition of the surface exhibited a Ca:Ti:P atomic ratio of 1.0:3.9:5.1 and found that after acid etching of the glass-ceramic, the phase that leached out of a $CaTi_4(PO_4)_6$ phase was apatite that formed preferentially in the presence of fluorine. The micrographs of the glass-ceramics in the present study showed very similar morphology, however the XRD analysis did not show any evidence of apatite formation. This unfortunately does not make the

explanation of the present ESEM study easier. In addition, all glass-ceramics exhibited clear lack of fluorine as it seems that all fluorine escapes during treatment in the form of CaF_2. It is believed, that if apatite was present, the crystal size would have been very small and not possible to detect by XRD. This is only an assumption and further work is necessary to be conducted in order to prove the above explanation. Furthermore, the micrographs showed that different crystal phases were present in both types of glass-ceramics. In the type A glass-ceramics, the addition of TiO_2 for CaF_2 resulted in a rough surface and a spherical morphology in the case of $CPFTR_3$ which is attributed to titanium pyro-phosphate surface crystallisation. The morphology in the type B glass-ceramics is different to the morphology of its surface and it is evident that there is a crystal phase which is crystallised on the surface of the glass-ceramic. In both types of glass-ceramics, the independent pits showed crystals inside with certain orientation. Moreover, in the bulk the crystals with certain orientation are both attributed to meta-phosphate and pyro-phosphate phases.

4.8 Energy Dispersive X-ray Analysis

EDX analysis conducted on type A and B glasses and glass-ceramics surface are shown in tables 3.14 to 3.17, which give information on the real glass compositions after they were made, as well giving information on the glass compositions after heat treatment.

For the type A glasses (table 3.14), fluorine was retained as a small amount only in glass $CPFTR_3$ (15 mol % TiO_2) and was not retained in glass $CPFTR_2$ (5 mol % TiO_2) and in the type A glass-ceramics there was no fluorine retained at all in any of the crystallised glass samples (table 3.16).

For the type B glasses (table 3.15) it was found that fluorine was retained in only a small amount in glasses $CPCTA_2$ (11.11 mol % TiO_2), $CPCTA_3$ (16.66 mol % TiO_2) and $CPCTA_4$ (20 mol % TiO_2) and in the case of glass CPCTA, no fluorine was retained. For the type B glass-ceramics there was no fluorine retained at all (table 3.17).

Therefore a small amount of fluorine was retained only in some of the compositions and that these compositions where it was retained were only present in the amorphous glass. This suggests that fluorine does escape from the glass during glass making and during crystallisation. It is also worth noting that no fluorine containing crystalline phase was observed in any of the glass-ceramics. This suggestion of fluorine release is possibly be due to the fact that a large amount of P_2O_5 was used in the manufacturing of the glasses. Therefore a large amount of this oxide was used to make the glass, hence a possibility of calcium fluoride reacting with the H_2O molecules is highly probable due to P_2O_5 being hydrophilic in the reaction:

$$\mathbf{CaF_2 + 2H_2O \rightarrow Ca(OH)_2 + 2HF}$$

Therefore fluorine would escape as hydrofluoric acid and so fluorine would not be present in the crystallised glass.

Furthermore, although APS took place in the glasses this was not evident from EDX as the scale of the volume analysed by EDX was much larger than the scale of APS.

CHAPTER 5

5. Conclusions

The effect of TiO_2 addition with reduction of calcium to phosphorus ratio (Ca/P = ≤0.5) and TiO_2 addition with constant calcium to phosphorus ratio (Ca/P = 0.5) on the structure of fluorine containing calcium phosphate glasses and glass-ceramics was demonstrated in the present study. The glasses were produced via a melting route and then were quenched on a stainless steel plate. A calcium phosphate glass which did not contain TiO_2 or CaF_2 was used as a reference throughout this study. In type A glasses whereby the Ca/P was reduced to ≤0.5, the TiO_2 addition for CaF_2 took place in 5 %, 15 % and 20 % molar content of TiO_2 and in type B glasses whereby there was a constant Ca/P of 0.5, TiO_2 addition took place in 4.76 %, 11.11 %, 16.66 % and 20 % molar content of TiO_2.

Glass $CPFTR_4$ whereby 20 % TiO_2 was added could not be produced. All the other glasses could be produced and DSC, XRD, FTIR, ESEM and TGA (performed only on amorphous glasses only) were used to characterise these in order to see the effect of TiO_2 addition on the structure and crystallisation of the glasses. Moreover, density and oxygen density measurements were taken to see the effect of TiO_2 on the glass-network.

DSC analysis demonstrated that in type A glasses, the Tg increased when TiO_2 was added up to 5 % however when 15 % TiO_2 was added there was a significant decrease which showed that addition of 15 % TiO_2 causes disruption in the glass network. There was a similar trend observed for the Tp values for these glasses and for the Tm glasses there was not an overall significant change in the values. As for the type B glasses, there was a general increase in both the Tg's except in the case of addition of 16.66 % TiO_2 whereby a decrease was observed. The general increase was expected

due to the fact that TiO_2 is known to increase the glass viscosity and strengthen the glass network and as for the decrease as it was less than 25°C it was attributed to the two amorphous phases present in the glass. The trend for the Tp values was similar and it was shown that titanium pyrophosphate had a significant effect on the glass, which was demonstrated by the change in Tp. The Tm values did not have an overall significant change, just as in the type A glasses.

The density results showed that in both type A and B glasses, addition of TiO_2 caused a general increase in density of glasses and that and this was expected due to Ti having a larger atomic weight, larger electrical charge and a smaller ionic radius than Ca. Furthermore the oxygen density results showed that TiO_2 addition in type A glasses caused a slight decrease in the oxygen density which suggested that Ti causes some disruption in the glass network. However TiO_2 addition in the type B glasses caused the oxygen density values to slightly increase and because these values were of minor change, it was suggested that TiO_2 addition in type B glasses does not have a significant effect on the glass network.

XRD analysis showed that in both the type A and B glass-ceramics; crystal phases corresponding to calcium metaphosphate as the main phase and calcium pyrophosphate and titanium pyrophosphate as secondary phases were observed. In the case of the calcium phosphate glass without TiO_2 or CaF_2, only the calcium metaphosphate phase was present as the main phase. No phase corresponding to fluorine was observed in any of the XRD patterns of the glass-ceramics.

FTIR spectra of the type A and B glasses showed a lack of peaks overall which confirmed that there was disorder in the phosphate network. Both the spectra showed peaks corresponding to the metaphosphate, pyrophosphate and orthophosphate

groups. In the spectra of both types of glass-ceramics peaks corresponding to the metaphosphate and pyrophosphate groups were decomposed into several narrow peaks in the spectra of the glass-ceramics. Furthermore there were no peaks relating to Ti-O-Ti linkages, which suggested that titanium ions were consumed during the formation of a crystalline phase such as TiP_2O_7, confirmed by XRD patterns.

ESEM images demonstrated the presence of different crystal phases in the glass-ceramics. Titanium pyrophosphate was seen at the surface of the glass-ceramics and in the bulk of the glass-ceramics, crystals corresponding to metaphosphate and pyrophosphate were observed.

From TGA analysis, we did not expect to see mass reduction of the amorphous type A and B glasses, however significant mass reduction was observed in type A glass $CPFTR_2$, containing 5 mol % TiO_2. It was expected for fluorine to be retained in all the glass samples. However from TGA and EDX analysis it was evident that a small amount of fluorine was only retained in the amorphous glasses except in the case of glass $CPFTR_2$ (5 % TiO_2) and CPCTA (4.76 % TiO_2), and fluorine was not present in any of the crystallised glass samples (confirmed by XRD patterns) which suggests that fluorine escapes from the glass most probably as hydrofluoric acid.

References

1. Rheinberger, V, Schweiger, M, & Holand, W. (2003). Control of nucleation in glass-ceramics. Philosophical transactions - Royal Society. Mathematical, Physical and engineering sciences, **361**(1804), 575-588.

2. Holland W, Beall G. (2002). Glass-Ceramic Technology, The American Ceramic Society, Westerville, OH

3. Strnad Z. (1986). Glass-Ceramic Materials: liquid phase separation, nucleation, and crystallization in glasses, Elsevier, Amsterdam.

4. M^{c}Millan P W. (1979). Glass-Ceramics: Non-Metallic Solids, 2nd edn. Academic Press Inc, London, pp 1-5, 100-110.

5. Burgner L L, Weinberg M C. (2001). Crystal growth mechanisms in inorganic glasses, Physics and Chemistry of Glasses, vol. 42, pp. 184-190.

6. Shelby J E. (1997). Introduction to Glass Science and Technology (RSC paperbacks), The Royal Society of Chemistry, pp 1-68

7. Cahn J W, Charles R J. (1965) Initial Stages of Phase Separation In Glasses, Physics And Chemistry Of Glasses, vol. 6, pp. 181-191.

8. Wu, J, Boccaccini, A, & Rawlings, R. (2006). Glass-ceramics: Their production from wastes-a review. Journal of materials science, **41**(3), 733-761.

9. Schweiger, M, Rheinberger, V, Kappert, H. (2009). Bioceramics and their application for dental restoration. Advances in Applied Ceramics, **108**(6), 373-380.

10. Stookey, S. (1959). Catalyzed crystallization of glass in theory and practice. Industrial & engineering chemistry, **51**(7), 805-808.

11. Beall, G. (1992). Design and properties of glass-ceramics. Annual review of materials science, **22**, 91-119.

12. Rheinberger, V, Apel, E. (2006). Clinical applications of glass-ceramics in dentistry. Journal of materials science. Materials in medicine, **17**(11), 1037-1042.

13. Kokuba T. (2008). Bioceramics and their clinical applications, Japan Medical Materials, Woodhead publishing, Cambridge, pp 548-566

14. Denry, I. (1996). Recent advances in ceramics for dentistry. Critical reviews in oral biology and medicine, **7**(2), 134-143.

15. Best, S, Porter, A, Thian, E. (2008). Bioceramics: Past, present and for the future. Journal of the European Ceramic Society, **28**(7), 1319-1327.

16. Hench, L L. (1971). Bonding Mechanisms at the Interface of Ceramic Prosthetic Materials. Biomedical Materials Research, **2**, 117-141.

17. Kokubo T, Shigematsu M, Nagashima Y, Tashiro M, Nakamura, T,Yamamuro T, Higashi S. (1982). Apatite- and Wollastonite-containing glass-ceramics for

prosthetic applications, Bulletin of the Institute for Chemical Research, Kyoto University, pp. 260–268.

18. Albee, F. (1920). Studies in bone growth - Triple calcium phosphate as a stimulus osteogenesis. Annals of surgery, **71**, 32-39.

19. Levitt, G. E. (1969). Forming Methods for Apatite Prosthesis. Biomedical Materials Research, **3**, 683-685

20. Votava, W, Bass, D, M^{c}Mullen, J. (1971). New calcium phosphate ceramic material for bone and tooth implants. Journal of Dental Research, **50**(4), 860

21. Nery, Lynch, K, Hirthe, W, Mueller, K. (1975). Bioceramic implants in surgically produced infrabony defects. Journal of periodontology, **46**(6), 328-347.

22. LeGeros, R Z. (1988). Calcium phosphate materials in restorative dentistry: A review. Advances in dental research, **2**(1), 164-80.

23. Peitl, O, Zanotto, E, & Hench, L. (2001). Highly bioactive P_2O_5-Na_2O-CaO-SiO_2 glass-ceramics. Journal of non-crystalline solids, **292**(1-3), 115-126.

24. Franks, K, Abrahams, I, & Knowles, J. (2000). Development of soluble glasses for biomedical use part i: In vitro solubility measurement. Journal of materials science. Materials in medicine, **11**(10), 609-614.

25. Hench, L. (1998). Bioceramics. Journal of the American Ceramic Society, **81**(7), 1705-1728.

26. Navarro M, Ginebra M, Clement J. (2003). Physicochemical degradation of titania-stabilized soluble phosphate glasses for medical applications. Journal of the American Ceramic Society, **86**(8), 1345-1352.

27. Dias, A G. (2005). In situ thermal and structural characterization of bioactive calcium phosphate glass-ceramics containing TiO_2 and MgO oxides: High temperature–XRD studies. Journal of non-crystalline solids, **351**(10-11), 810.

28. Kitsugi, T, Yamamuro, T, Nakamura, T. (1995). Transmission electron-microscopy observations at the interface of bone and 4 types of calcium-phosphate ceramics with different calcium phosphorus molar ratios. Biomaterials, **16**(14), 1101-1107.

29. Gimenez, I, Mazali, I, & Alves, O. (2001). Application of Raman spectroscopy to the study of the phase composition of phosphate based glass-ceramics. The Journal of physics and chemistry of solids, **62**(7), 1251-1255.

30. Ryu, H, Youn, H, Hong, K. (2002). An improvement in sintering property of beta-tricalcium phosphate by addition of calcium pyrophosphate. Biomaterials, **23**(3), 909-914.

31. Dias, A G. (2007). Physicochemical degradation studies of calcium phosphate glass-ceramic in the $CaO–P_2O_5–MgO–TiO_2$ system. Acta Biomaterialia, **3**(2), 263.

32. Chun, S, Na, S, Lee, J. (2002). Biodegradation study of potassium calcium metaphosphate in the SBF and tris-buffer solution. Key engineering materials, Bioceramics **14**. (218-220), 149-152.

33. Kasuga, T. (1999). Bioactive ceramics prepared by sintering and crystallization of calcium phosphate invert glasses. Biomaterials, **20**(15), 1415-1420.

34. Zhang, Y. (2001). Microstructural characterization and in vitro apatite formation in $CaO–P_2O_5–TiO_2–MgO–Na_2O$ glass-ceramics. Journal of the European Ceramic Society, **21**(2), 169.

35. Kasuga, T. (1998). Novel calcium phosphate ceramics prepared by powder sintering and crystallization of glasses in the pyrophosphate region. Journal of Materials Research, **13**(12), 3357-3360.

36. Kasuga, T. (1999). Calcium phosphate invert glasses with soda and titania. Journal of Non-Crystalline Solids, **243**(1), 70-74.

37. Kasuga, T. (2001). Machinable calcium pyrophosphate glass-ceramics. Journal of Materials Research, **16**(3), 876-880.

38. Kasuga, T, Nogami, M, & Niinomi, M. (2003). Calcium phosphate glass-ceramics for bioactive coating on a beta-titanium alloy. Advanced Engineering Materials, **5**(7), 498-501.

39. Kasuga T, Nogami M, Hattori T. (2002). Preparation of calcium phosphate invert glass-ceramics with bioactivity and their coating on titanium alloys. Glass Science and Technology, **75**, 338-341.

40. Koo J, Bae B, & Na H. (1997). Raman spectroscopy of copper phosphate glasses. Journal of Non-Crystalline Solids, **212**(2-3), 173-179.

41. Kasuga T, Ueno E & Obata A. (2007). Preparation of apatite-containing calcium phosphate glass-ceramics. Key Engineering Materials, Bioceramics, **19**, pts 1 and 2, 330-332, 157-160.

42. Kasuga T, Kimata T & Obata A. (2009). Preparation of a calcium titanium phosphate glass-ceramic with improved chemical durability. Journal of the American Ceramic Society, **92**(8), 1709-1712.

43. Hosono H, Zhang Z & Abe Y. (1989). Porous glass-ceramic in the CaO-TiO_2-P_2O_5 system. Journal of the American Ceramic Society, **72**(9), 1587-1590.

44. Hosono H & Abe Y. (1995). Porous glass-ceramics composed of a titanium phosphate crystal skeleton - A review. Journal of Non-Crystalline Solids, **190**(3), 185-197.

45. Lee J S. (1999). The devitrification behavior of calcium phosphate glass with TiO_2 addition. Thermochimica Acta, **333** (2), 115.

46. Kishioka A, Haba M & Amagasa M. (1974). Glass formation in multicomponent phosphate systems containing TiO_2. Bulletin of the Chemical Society of Japan, **47**(10), 2493-2496.

47. Neel E A, Chrzanowski W & Knowles J. (2008). Effect of increasing titanium dioxide content on bulk and surface properties of phosphate-based glasses. Acta Biomaterialia, **4**(3), 523-534.

48. Brauer D. (2007). Solubility of glasses in the system P_2O_5-CaO-MgO-Na_2O-TiO_2: Experimental and modelling using artificial neural networks. Journal of Non-Crystalline Solids, **353**(3), 263-270.

49. Aoki H. (1994). Medical applications of hydroxyapatite: bone mineral, drug delivery system, cancer & HIV, IVH & CAPD, dental implant, Ishiyaku EuroAmerica, Tokyo pp 286-306.

50. Abo-Naf S, El-Amiry M & Abdel-Khalek A. (2008). FTIR and UV-VIS optical absorption spectra of gamma-irradiated calcium phosphate glasses doped with Cr_2O_3, V_2O_5 and Fe_2O_3. Optical Materials, **30**(6), 900-909.

51. El-Batal F. (2009). UV-Visible, Infrared, Raman and ESR spectra of gamma-irradiated TiO_2-doped soda lime phosphate glasses. Indian journal of pure & applied physics, **47**(9), 631-642.

52. Neel E A, Chrzanowski W, Valappil. (2009). Doping of a high calcium oxide metaphosphate glass with titanium dioxide. Journal of non-crystalline solids, **355**(16-17), 991-1000.

53. Cai S, Zhang W, Xu G. (2009). Microstructural characteristics and crystallization of CaO-P_2O_5-Na_2O-ZnO glass-ceramics prepared by sol-gel method. Journal of non-crystalline solids, **355**(4-5), 273-279.

54. Shaim, A & Et-tabirou M. (2003). Role of titanium in sodium titanophosphate glasses and a model of structural units. Materials chemistry and physics, **80**(1), 63-67.

55. Krishna G, Veeraiah N, Venkatramaiah N. (2008). Induced crystallization and physical properties of Li_2O-CaF_2-P_2O_5-TiO_2 glass system - Part i. characterization, spectroscopic and elastic properties. Journal of alloys and compounds, **450**(1-2), 477-485.

56. Pattanayak D K. (2003). Synthesis and Characterisation of Titanium-Calcium Phosphate composites for bio applications. Trends biomaterials artificial organs, **17** (1), 8-12

57. Dias A. (2003). In vitro degradation studies of calcium phosphate glass-ceramics prepared by controlled crystallization. Journal of non-crystalline solids, **330**(1-3), 81-89.

58. Freeman C O, Brook I M, Johnson A, Hatton P V, Hill R G. (2003) Crystallization modifies osteoconductivity in an apatite–mullite glass–ceramic, Journal of Materials Science: Materials in Medicine, **14**, 985-990.

59. Griffin S G, Hill R G.. (2000) Influence of glass composition on the properties of glass polyalkenoate cements. Part IV: influence of fluorine content, Biomaterials, **21**, 693-698.

60. Hill R, Wood D, Thomas M. (1999). Trimethylsilylation analysis of the silicate structure of fluoro-alumino-silicate glasses and the structural role of fluorine, Journal of Materials Science, **34**, 1767-1774.

61. Wilson D A, Crisp S, Prosser H J, Lewis B G, Merson S A. (1980). Aluminosilicate Glasses For Poly-Electrolyte Cements, Industrial & Engineering Chemistry Product Research And Development, **19**, 263-270.

62. Hill R G, Wilson D A, (1988). Some structural aspects of glasses used in ionomer cements, Glass Technology, **29**, 150-157.

63. Zeng Q, Stebbins J F. (2000). Fluoride sites in aluminosilicate glasses: High-resolution F-19 NMR results, American Mineralogist, **85**, 863-867.

64. Stebbins J F, Kroeker S, Lee S K, Kiczenski T J. (2000) Quantification of five- and six-coordinated aluminum ions in aluminosilicate and fluoride-containing glasses by high-field, high-resolution Al-27 NMR, Journal of Non-Crystalline Solids, **275**, 1-6.

65. Clifford A, Rafferty A, Hill R, Mooney P, Wood D, Samuneva B, Matsuya S, (2001) The influence of calcium to phosphate ratio on the nucleation and crystallisation of apatite glass ceramics, Journal of Materials Science: Materials in Medicine, **12**, 461-469.

66. Rafferty A, Clifford A, Hill R, Wood D, Samuneva B, Dimitrova-Lukacs M. (2000) Influence of fluorine content in apatite-mullite glass ceramics, Journal of the American Ceramic Society, **83**, 2833-2838.